

Liquidus of Silicon Binary Systems

JAFAR SAFARIAN, LEIV KOLBEINSEN, and MERETE TANGSTAD

Thermodynamic knowledge about liquid silicon is crucial for the production of solar-grade silicon feedstock from molten silicon. In the current study, liquidus for silicon binary alloys is formulated using a previously developed method in which the liquidus curve is calculated using two constants. The liquidus measurements for the silicon portion of the silicon alloys with Al, Ca, Mg, Fe, Ti, Zn, Cu, Ag, Au, Pt, Sn, Pb, Bi, Sb, Ga, In, Ni, Pd, Mn, and Rh are reviewed, and the consistent data were used to determine the liquidus constants. The liquidus curves for silicon binary systems are calculated and plotted. It is indicated that the calculated liquidus curves fit well with the experimental data. A correlation between the determined liquidus constants is also observed, which can be used to gain a better understanding of the thermodynamics of the silicon binary melts.

DOI: 10.1007/s11663-011-9507-4

© The Author(s) 2011. This article is published with open access at Springerlink.com

I. INTRODUCTION

SILICON is used as a raw material for the chemical and semiconductor industries, and also as an alloying element in the production of metals such as aluminum and steel production.^[1] With regard to the rapid growth of the photovoltaic industry since the 2000s, it is predicted that silicon will be important in 21st century, playing a key role in the energy production by silicon solar cells. Silicon is produced from quartz through a carbothermic reduction in electric arc furnaces, and the product, which is called metallurgical-grade silicon (MG-Si), contains approximately 1 wt pct impurities. Because MG-Si is used to produce solar grade silicon (SoG-Si) with more than 99.9999 wt pct Si, its refining is necessary. The most economic silicon purification processes to gain SoG-Si are expected to be those involving liquid silicon treatment. Therefore, thermodynamic knowledge about the behavior of solute elements in liquid silicon is crucially important.

The scope of the current study is to study the liquidus in the silicon portion of silicon binary systems with regard to the available experimental data. Liquidus information is important with regard to paving the way to understanding the behavior of molten silicon and solute elements in silicon. The thermodynamic properties of the molten alloys such as activities of the melt components can be calculated through the liquidus data. Activities in silicon binary melts have been studied previously by the authors and the results will be published separately.

II. REVIEW OF LIQUIDUS THERMODYNAMICS

Considering a binary system of Si-Me with solid solubility of Me in Si, the liquidus on silicon side is described as^[2]:

$$RT \ln \left(\frac{a_{\text{Si}}^{\text{l}}}{a_{\text{Si}}^{\text{ss}}} \right) = -\Delta G_{f,\text{Si}}^{\circ} \quad [1]$$

where a_{Si}^{l} and $a_{\text{Si}}^{\text{ss}}$ are the activities of silicon in liquid and solid solution phases at temperature T , respectively. R is the universal gas constant and $\Delta G_{f,\text{Si}}^{\circ}$ is the Gibbs free energy change from the fusion of silicon. The changes in the heat capacity through silicon fusion is a function of temperature in the form of $\Delta C_p = a + bT + c/T^2$, according to the available data,^[3] $a = 1.67$, $b = -2.47 \times 10^{-3}$ and $c = 4.14 \times 10^5 \text{ J}\cdot\text{mol}^{-1}\cdot\text{K}^{-1}$. The change of ΔC_p in a wide temperature range below the silicon melting point is small and negligible. Assuming $\Delta C_p \approx 0$, Eq. [1] can be written as:

$$\ln \left(\frac{a_{\text{Si}}^{\text{l}}}{a_{\text{Si}}^{\text{ss}}} \right) = -\frac{\Delta H_{f,\text{Si}}^{\circ}}{R} \left(\frac{1}{T} - \frac{1}{T_{f,\text{Si}}} \right) \quad [2]$$

where $\Delta H_{f,\text{Si}}^{\circ}$ and $T_{f,\text{Si}}$ are the change in the enthalpy of fusion of silicon and fusion temperature, respectively. Because the activity of solution components is a function of the chemical composition, we obtain Eq. [3]:

$$\ln \left(\frac{\gamma_{\text{Si}}^{\text{l}} X_{\text{Si}}^{\text{l}}}{\gamma_{\text{Si}}^{\text{ss}} X_{\text{Si}}^{\text{ss}}} \right) = -\frac{\Delta H_{f,\text{Si}}^{\circ}}{R} \left(\frac{1}{T} - \frac{1}{T_{f,\text{Si}}} \right) \quad [3]$$

where γ_{Si} is the activity coefficient and X_{Si} is the mole fraction of silicon. Considering negligible solid solubility of Me in silicon ($a_{\text{Si}}^{\text{ss}} \approx 1$), Eq. [3] is simplified:

$$\ln \gamma_{\text{Si}}^{\text{l}} X_{\text{Si}}^{\text{l}} = -\frac{\Delta H_{f,\text{Si}}^{\circ}}{R} \left(\frac{1}{T} - \frac{1}{T_{f,\text{Si}}} \right) \quad [4]$$

In principle, the relationship between the activity coefficient of solution component such as silicon here and other thermodynamic parameters is expressed as:

JAFAR SAFARIAN, Research Scientist, and LEIV KOLBEINSEN and MERETE TANGSTAD, Professors, are with the Department of Materials Science and Engineering, Norwegian University of Science and Technology, NO 7491, Trondheim, Norway. Contact e-mail: Jafar.Safarian@material.ntnu.no

Manuscript submitted February 25, 2011.

Article published online April 2, 2011.

$$RT \ln \gamma_{\text{Si}}^1 = \Delta \bar{G}_{\text{Si}}^e = \Delta \bar{H}_{\text{Si}} - T \Delta \bar{S}_{\text{Si}}^e \quad [5]$$

where $\Delta \bar{G}_{\text{Si}}^e$, $\Delta \bar{H}_{\text{Si}}$, and $\Delta \bar{S}_{\text{Si}}^e$ are the relative partial molar excess free energy, the relative partial molar excess enthalpy of solution, and the relative partial molar excess entropy of silicon, respectively. Parameters $\Delta \bar{H}_{\text{Si}}$ and $\Delta \bar{S}_{\text{Si}}^e$ are in principle dependent on the temperature and composition, and the effect of temperature is negligible compared with composition. It has been shown that they can be expressed as follows^[4]:

$$\Delta \bar{H}_{\text{Si}} = a(1 - X_{\text{Si}}^1)^2 \quad [6]$$

$$\Delta \bar{S}_{\text{Si}}^e = b(1 - X_{\text{Si}}^1)^2 \quad [7]$$

where a and b are constants independent of temperature and composition. Combining Eqs. [4] and [5] and regarding Eqs. [6] and [7], a parameter called α can be defined.^[4] This parameter can be calculated for every individual solubility measurement according to Eq. [8]

$$\alpha \equiv \frac{RT \ln \gamma_{\text{Si}}^1}{(1 - X_{\text{Si}}^1)^2} = \frac{T \Delta S_{f,\text{Si}}^\circ - \Delta H_{f,\text{Si}}^\circ - RT \ln X_{\text{Si}}^1}{(1 - X_{\text{Si}}^1)^2} = a - bT \quad [8]$$

where $\Delta S_{f,\text{Si}}^\circ$ is the entropy of fusion of silicon. Every individual liquidus measurement on the silicon portion of a binary system can be used to determine an individual α value by the middle part of Eq. [8]. A plot of α values for different liquidus coordinates against the corresponding temperatures shows usually a linear relationship, and therefore, the liquidus constants a and b can be determined graphically. The liquidus temperature of the binary system on the silicon portion can accordingly be calculated by Eq. [9], which is obtained through the rearrangement of Eq. [8]:

$$T = \frac{\Delta H_{f,\text{Si}}^\circ + a(1 - X_{\text{Si}}^1)^2}{\Delta S_{f,\text{Si}}^\circ - R \ln X_{\text{Si}}^1 + b(1 - X_{\text{Si}}^1)^2} \quad [9]$$

Liquidus constants for silicon binary systems with Al, Ga, In, Tl, Sn, As, Sb, Bi, Cu, Ag, Au, and Zn were determined using this method by Thurmond and Kowalchik in 1960.^[4] Because much experimental data on many of these systems have been reported since the 1970s, their liquidus constants are recalculated in the current study. Moreover, the liquidus constants for the silicon binary systems with Ca, Mg, Fe, Ti, Pd, Ni, Mn, and Rh are calculated. Furthermore, the liquidus curves are calculated and compared with the experimental data graphically. It is worth noting that the current study does not cover systems with considerable solid solubility in silicon at high temperatures such as boron, phosphorus, and arsenic.

III. LIQUIDUS CALCULATION

An overall view of 20 silicon binary systems is presented in this section with focus on the liquidus

range on the silicon portion. The liquidus measurements in the literature are evaluated and the consistent data are used to determine the liquidus constants a and b . In addition, the liquidus curves are calculated using Eq. [9], and the results are graphically plotted and compared with the experimentally determined liquidus coordinates.

A. Si-Al System

The equilibrium diagram of Si-Al is a simple eutectic system with two solid solution phases. There is a eutectic in this system at 850.1 K (577.1 °C) and $X_{\text{Si}} = 0.122$.^[5] The liquidus of this system has been measured through many experimental works,^[6–16] which had been mostly done using thermal analysis. The measured liquidus for Si-Al system from several studies are listed in Table I for both hypoeutectic and hypereutectic compositions to clear the liquidus calculation procedure. The liquidus data for the other silicon binary systems are not tabulated here as they are shown in the related phase diagrams.

A plot of the calculated α values by Eq. [8] from the liquidus data on the silicon portion (Table I) is shown in Figure 1. For calculations, $\Delta H_{f,\text{Si}}^\circ = 50654.3$ J/mol was considered, which gives $\Delta S_{f,\text{Si}}^\circ = 30.026$ J/mol-K regarding $T_{f,\text{Si}} = 1687$ K.^[3] Parameter α is sensitive to error in T and X_{Si} near the melting point.^[4] Therefore, the data close to the silicon melting point are not used here to calculate α values; these data are marked by star symbol * in Table I. The trend line in Figure 1 shows $a = -9789.7$ J/mol and $b = 3.74$ J/mol-K. These constants are different from the previously calculated values as $a = -17322.6$ J/mol and $b = -5.1$ J/mol-K^[4] because of the use of more experimental data. Substitution of these liquidus constants in Eq. [9] the liquidus curve on silicon side is calculated as shown Figure 2. Obviously, there is a good correlation between the calculated liquidus and the experimental measurements even for the experimental points in Table I that were not used to determine the liquidus constants.

The liquidus on the aluminum portion of the phase diagram (Figure 2) was also determined using the previously determined liquidus constant values. Equation 10, which can be obtained similar to Eq. [9], was used for the calculations considering $\Delta H_{f,\text{Al}}^\circ = 10,460.49$ J/mol, $T_{f,\text{Al}} = 932$ K (659 °C), and $\Delta S_{f,\text{Al}}^\circ = 11.22$ J/mol-K.^[3] The obtained liquidus curve fits well with the reported experimental data (Table I) for this portion of the phase diagram. This may indicate the proper accuracy of the determined liquidus constants.

$$T = \frac{\Delta H_{f,\text{Al}}^\circ + a(1 - X_{\text{Al}})^2}{\Delta S_{f,\text{Al}}^\circ - R \ln X_{\text{Al}} + b(1 - X_{\text{Al}})^2} \quad [10]$$

The calculated liquidus curve on silicon side (Figure 2) gives a eutectic composition as $X_{\text{Si}} = 0.119$ at $T = 850.1$ K (577.1 °C), which is close to other works as reviewed by Murray and McAlister.^[5]

Table I. The Measured Liquidus Data for Si-Al System^[6-16]

Reference	Liquidus Data on Si Side of the Eutectic		Liquidus Data on Al Side of the Eutectic	
	X_{Si}	Temperature, K (°C)	X_{Si}^*	Temperature, K (°C)*
Fraenkel ^[6]	0.194	957 (684)	—	—
	0.391	1232 (959)		
	0.597	1439 (1166)		
	0.717	1503 (1230)		
Roberts ^[7]	0.179	969 (696)	—	—
	0.319	1116 (843)		
	0.391	1232 (959)		
	0.482	1307 (1034)		
	0.698*	1503 (1230)*		
	0.731*	1526 (1253)*		
	0.850*	1607 (1334)*		
Gwyer and Phillips ^[8]	0.134	875 (602)	0.113	850 (577)
	0.142	889 (616)	0.116	852 (579)
	0.183	950 (677)	0.119	852 (579)
			0.124	867 (594)
Broniewski and Smailowski ^[9]	0.337	1131 (858)		
	0.51	1333 (1060)		
Matsuyama ^[10]	0.145	893 (620)	0.077	878 (605)
	0.194	957 (684)		
	0.292	1075 (802)		
	0.39	1188 (915)		
	0.49	1278 (1005)		
	0.59	1380 (1107)		
	0.692	1473 (1200)		
	0.794*	1545 (1272)*		
	0.896*	1640 (1367)*		
	Carighead <i>et al.</i> ^[12]	0.118	851 (578)	0.0472
0.123		854 (581)	0.0771	883 (610)
0.132		871 (598)	0.1079	857 (584)
Berthon <i>et al.</i> ^[13]	0.145	875 (602)	0.02	915 (642)
	0.165	905 (632)	0.048	901 (628)
	0.193	955 (682)	0.068	890 (617)
	0.213	982 (709)	0.096	871 (598)
	0.242	1015 (742)	0.116	853 (580)
	0.262	1039 (766)		
	0.291	1075 (802)		
	0.351	1160 (887)		
Kobayashi <i>et al.</i> ^[14,15]	0.194	973 (700)	0.058	894 (621)
			0.077	878.5 (605.5)
			0.096	861 (588)
Girault <i>et al.</i> ^[16]	0.13	873 (600)	—	—
	0.2	973 (700)		
	0.28	1073 (800)		
Singer and Cottrell ^[11]	—	—	0.0052	928 (655)
			0.0093	927 (654)
			0.0115	925 (652)
			0.0144	924 (651)
			0.0394	908 (635)
			0.078	881 (608)

*Data were not used to determine the liquidus constants.

B. Si-Ca System

In the Si-Ca binary system, there are intermediate compounds Ca_2Si , Ca_5Si_3 , $CaSi$, Ca_3Si_4 , $Ca_{14}Si_{19}$, and $CaSi_2$.^[17-20] The eutectic between silicon and $CaSi_2$ on the silicon portion is located at $T = 1293$ K (1020 °C) and $X_{Si} = 0.72$,^[20] 1296 K (1023 °C) and $X_{Si} = 0.69$,^[21] and 1253 K (980 °C) and $X_{Si} = 0.704$.^[22] The liquidus at higher silicon concentrations than eutectic has been

determined through measuring the total pressure over the Si-Ca liquids at different temperatures,^[21] thermal analysis, and electrical conductivity,^[22] using direct weighting Knudsen cell.^[23] The data of Tamaru^[24] are not considered here because the raw materials used contained large amounts of impurities.

The calculated α - T plot using literature liquidus data^[21-23] is shown in Figure 1; this plot gives liquidus

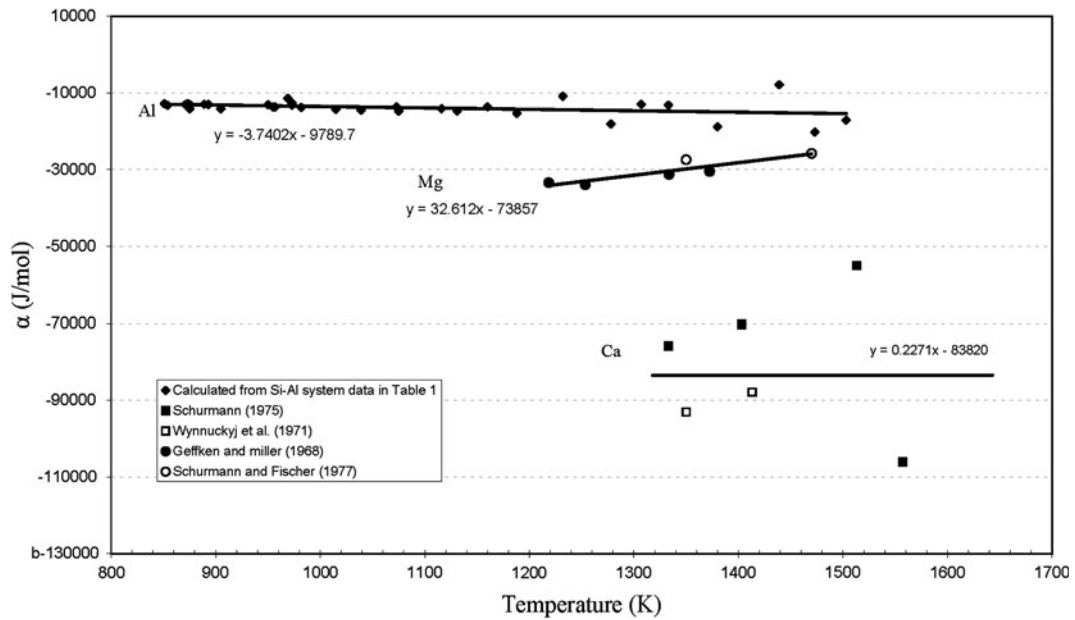


Fig. 1—The relationship between parameter α and temperature for Si-Al, Si-Ca, and Si-Mg systems.

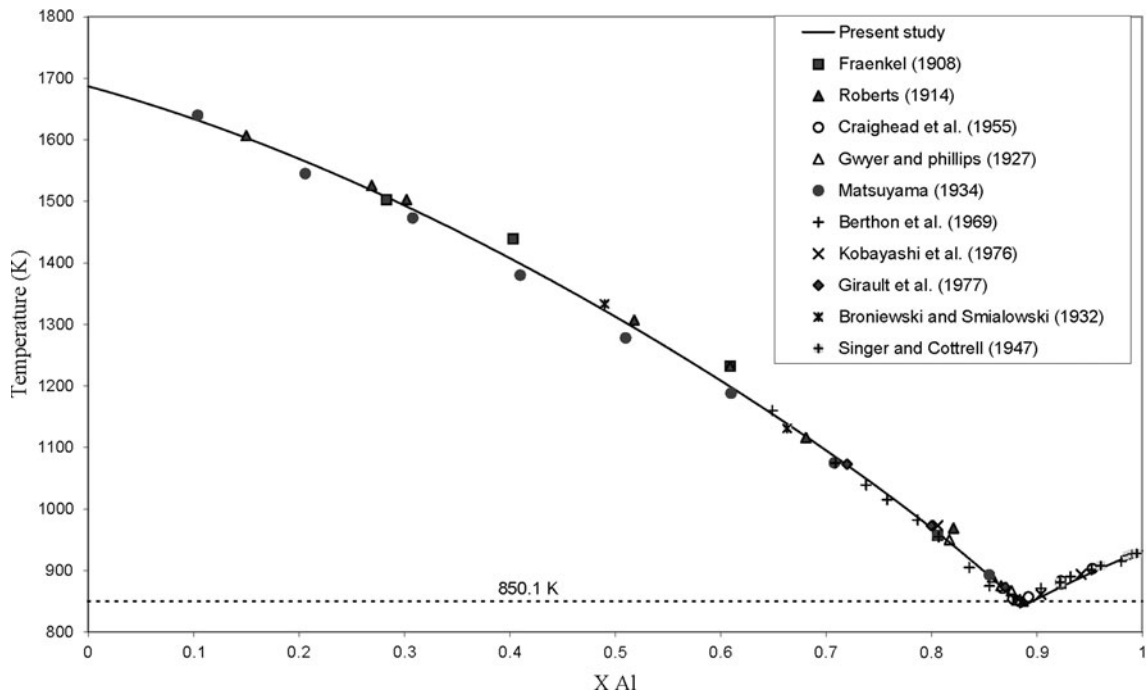


Fig. 2—The liquidus of Si-Al system.

constants $a = -83,820 \text{ J/mol}$ and $b = -0.23 \text{ J/mol-K}$. Considering these values, the liquidus on the silicon-rich part of Si-Ca system is calculated as shown by the solid curve in Figure 3. This curve predicts $X_{\text{Si}} = 0.694$ at 1296 K (1023 °C), which is close to the reported eutectic composition ($X_{\text{Si}} = 0.69$) by Schurmann *et al.*^[21]

C. Si-Mg System

The assessed phase diagram for the Si-Mg system contains an intermetallic compound Mg_2Si , and there is a

eutectic point between it and silicon with the coordinates of $T = 1217 \text{ K}$ (944 °C) and $X_{\text{Si}} = 0.53$.^[25,26] The liquidus between Mg_2Si and Si have been determined experimentally by Vogel^[27] using a thermal analysis, and by Wohler and Schliephake^[22] using a thermal analysis and electrical conductivity. Because there were considerable impurities in the materials they used, their data can be in low accuracy and they are not used in the current study. The liquidus data determined by Geffken and Miller^[28] using thermal analysis and those reported by Schurmann and Fischer^[29] are more consistent.

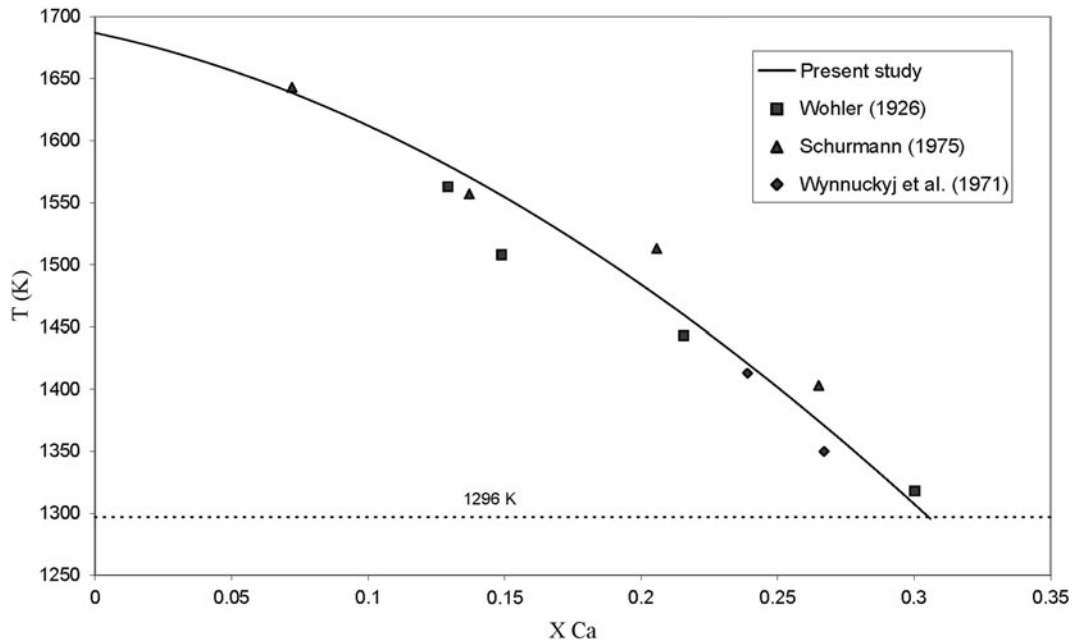


Fig. 3—The liquidus on the silicon portion of Si-Ca system.

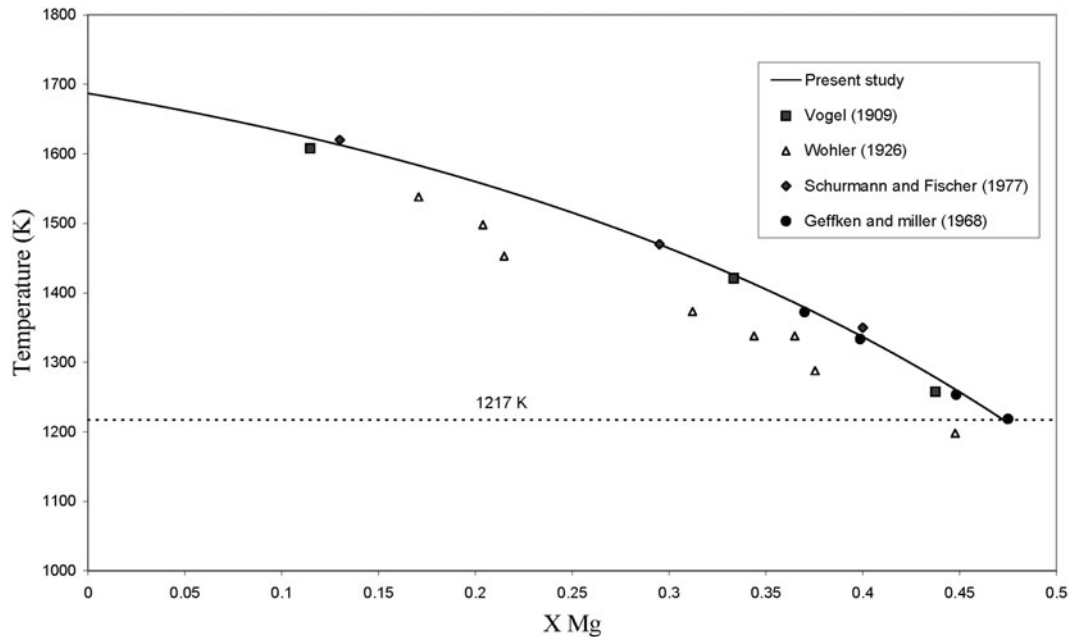


Fig. 4—The liquidus on the silicon portion of Si-Mg system.

The obtained α - T plot through treating the liquidus data for higher concentrations than the eutectic^[28,29] is shown in Figure 1, which gives liquidus constants $a = -73857$ J/mol and $b = -32.61$ J/mol-K. The calculated liquidus curve for the Si-Mg system and the reported liquidus values in literature are shown in Figure 4. It is observed that the calculated curve fits with the experimental data; however, it is above the old measurements done by Wohler and Schliephake.^[20] Their lower liquidus measurements may be related to the existence of considerable impurities in their material. The current calculated liquidus gives $X_{Si} = 0.527$ at

1217 K (944 °C), which is close to the reported eutectic composition by Yan *et al.*^[26]

D. Si-Fe System

The binary phase diagram for Fe-Si system contains intermediate phases between Si and Fe.^[30-36] A eutectic point on the silicon side of this system exists where liquid alloy is in equilibrium with Si and Fe_2Si_5 .^[37] This eutectic has been reported to be $X_{Si} = 0.735$ and 1207 °C.^[28-30] Eutectic temperatures at $T = 1481$ K and 1478 K (1208 °C and 1205 °C) have also been

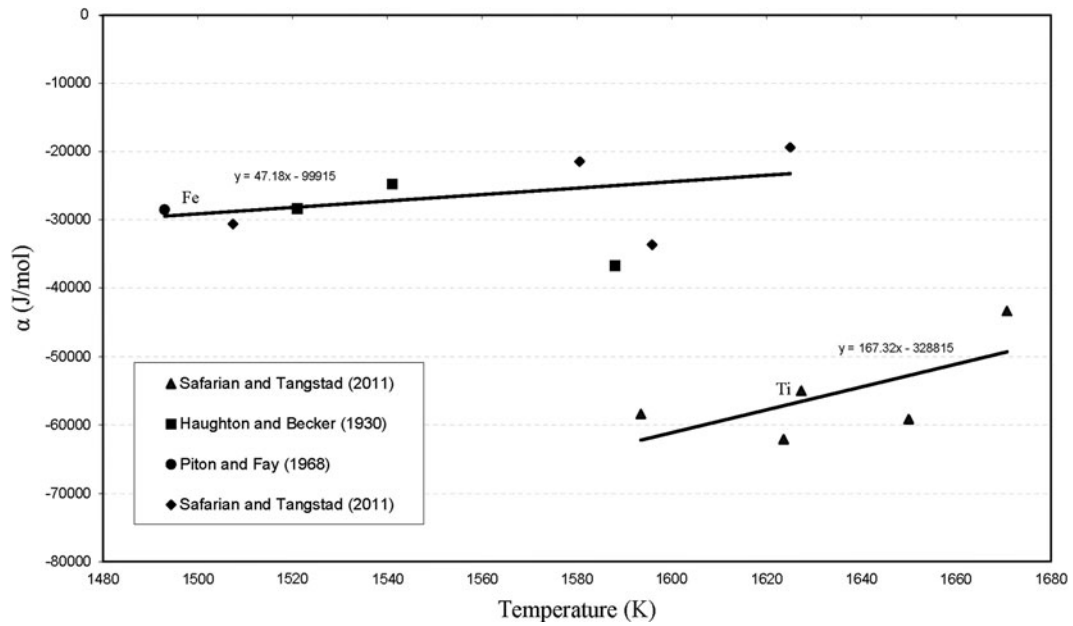


Fig. 5—The relationship between parameter α and temperature for Si-Fe and Si-Ti systems.

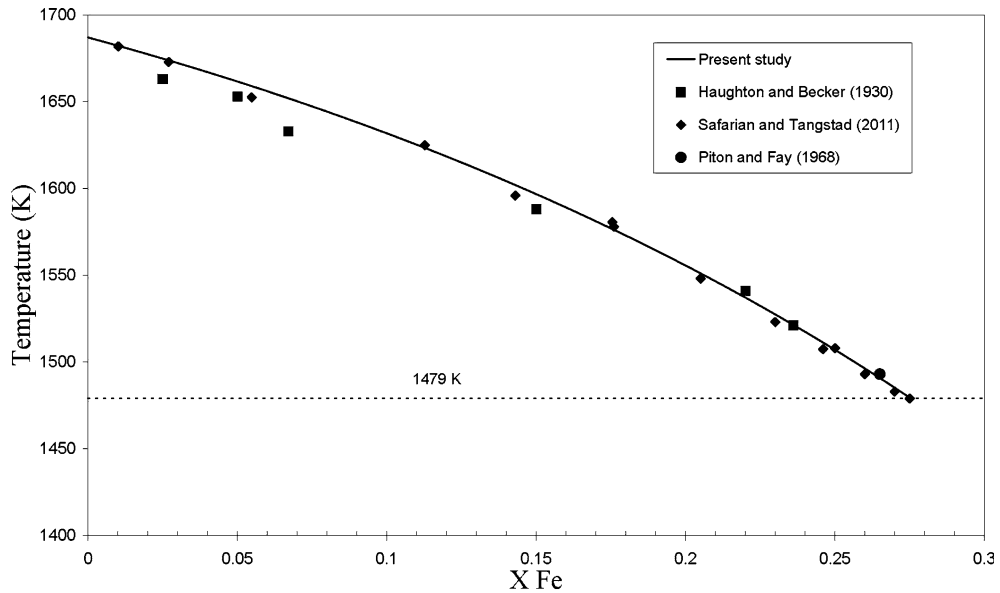


Fig. 6—The liquidus on the silicon portion of Si-Fe system.

determined through experimental works.^[33,34] Based on the recent study done by differential thermal analysis (DTA), the eutectic coordinates as $X_{\text{Si}} = 0.724$ and 1479 K (1206 °C) have been suggested by authors.^[37]

Based on the available liquidus data for the silicon side of the previous eutectic, the α values were calculated and plotted against temperature as shown in Figure 5. The trend line suggests liquidus constants $a = -99,915$ J/mol and $b = -47.18$ J/mol-K. For calculating the α values, the liquidus data close to the silicon melting point were not considered according to the explanation made in Section III-A. Figure 6 shows the calculated liquidus curve considering the preceding

liquidus constants using Eq. [9]. The obtained liquidus fits well with the experimental measurements. The calculated curve gives a eutectic composition $X_{\text{Si}} = 0.724$ at 1479 K (1206 °C), which is the same as the recently determined composition.^[37]

E. Si-Ti System

The Si-Ti binary phase diagram has been established through experimental studies^[38,39] with further assessment works.^[40-42] This system contains five titanium silicides TiSi_2 , TiSi , Ti_5Si_4 , Ti_5Si_3 , and Ti_3Si , and there is a eutectic reaction on the silicon side where a liquid is

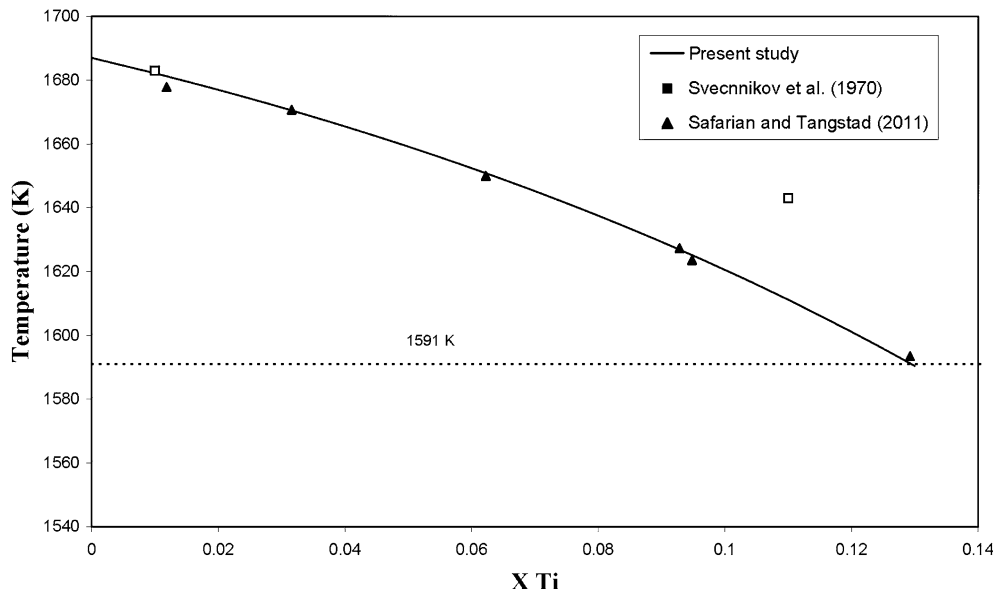


Fig. 7—The liquidus on the silicon portion of Si-Ti system.

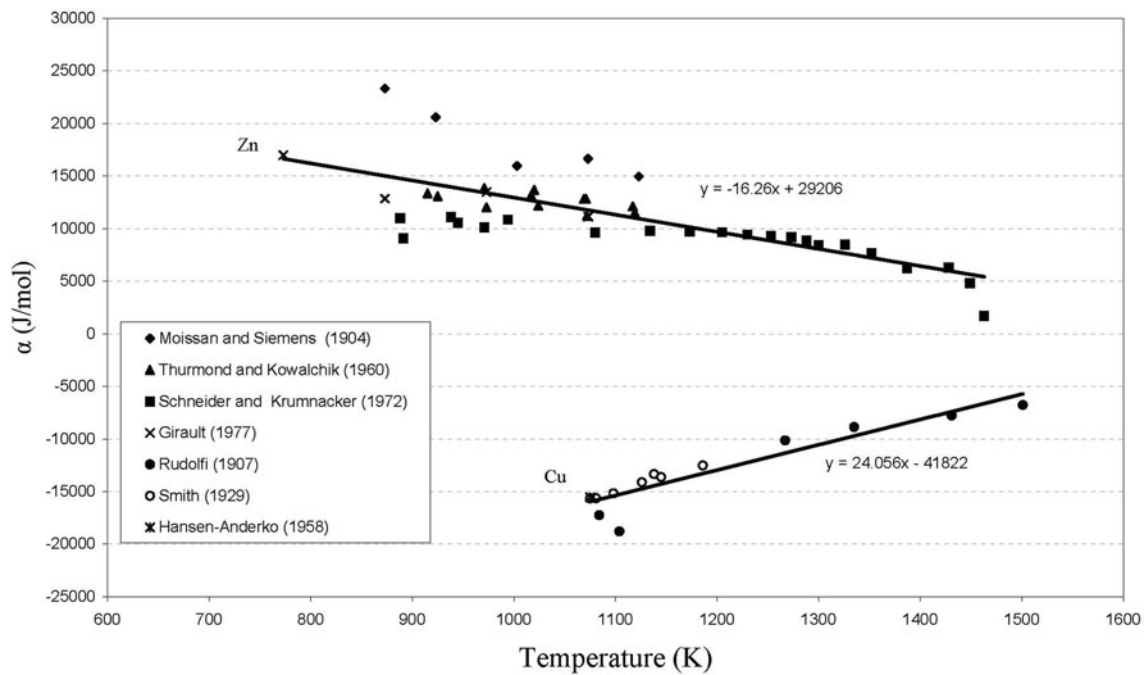


Fig. 8—The relationship between parameter α and temperature for Si-Zn and Si-Cu systems.

transformed to silicon and TiSi_2 . The recent reported coordinates for this eutectic are $X_{\text{Si}} = 0.868$ and 1591 K (1318 °C).^[37]

Liquidus constants for the silicon-rich part of Si-Ti system are obtained as $a = -328,815$ J/mol and $b = -167.32$ J/mol-K from the α - T plot of the liquidus data (Figure 5). The calculated liquidus using these constants is shown in Figure 7 by solid curve. As shown, there is a good correlation between the experimental data^[37] and the calculated liquidus. This liquidus gives a eutectic composition of $X_{\text{Si}} = 0.87$ at 1591 K (1318 °C), which is close to the experimentally determined eutectic point.

F. Si-Zn System

The Si-Zn phase diagram is a simple eutectic system with a eutectic at 692.2 K (419.2 °C) and $X_{\text{Si}} = 0.001$ according to the assessed phase diagram by Shukla *et al.*^[43] The liquidus of this system has been measured by gravimetric method^[4,16,44] and by differential thermal analysis (DTA).^[45,46]

Figure 8 shows the α - T plot using the reported liquidus data^[4,16,44,45] which gives $a = 29,206$ J/mol and $b = 16.26$ J/mol-K. These values are both greater than the previously reported values as $a = 17,980.36$ J/mol

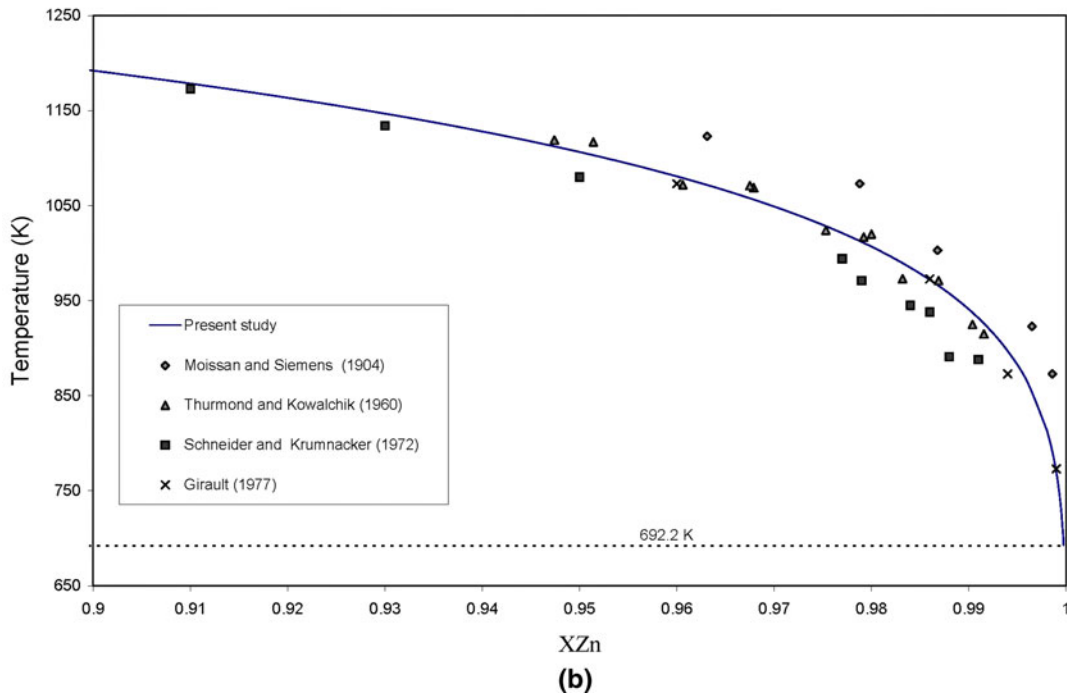
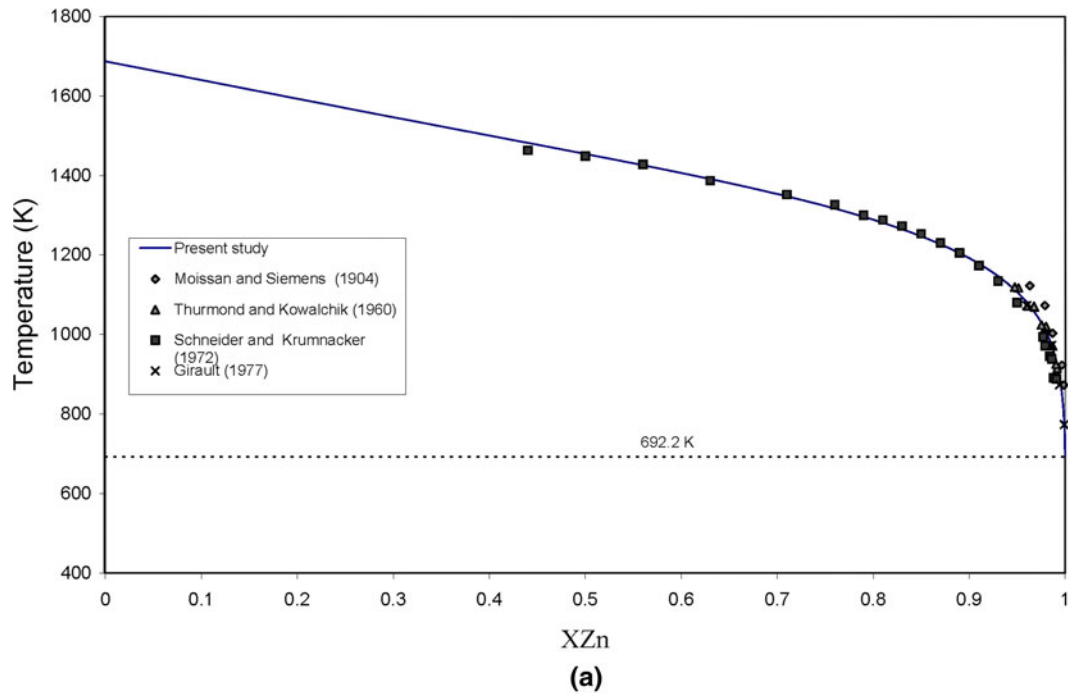


Fig. 9—The liquidus of Si-Zn system.

and $b = 4.77 \text{ J/mol-K}^{[4]}$ and $a = 20,980 \text{ J/mol}$ and $b = 9.20 \text{ J/mol-K}^{[47]}$. The calculated liquidus curve for this system using the obtained liquidus constants is shown in Figure 9. The calculated liquidus curve predicts $X_{\text{Si}} = 2.5 \times 10^{-4}$ at the eutectic temperature 692.2 K ($419.2 \text{ }^\circ\text{C}$), which is in lower silicon concentration than the previously calculated eutectic composition as $X_{\text{Si}} = 1 \times 10^{-3}^{[43]}$ and $X_{\text{Si}} = 4.5 \times 10^{-4}^{[47]}$.

G. Si-Cu System

In the Si-Cu binary system, a eutectic transformation from liquid to Si and $\text{Cu}_{19}\text{Si}_6$ exist at 1075 K ($802 \text{ }^\circ\text{C}$) with $X_{\text{Si}} = 0.301^{[48]}$ or $X_{\text{Si}} = 0.307^{[49]}$. The liquidus between this point and silicon has been measured by thermal analysis.^[50–52] These data were used to calculate the corresponding α values, which are shown in Figure 9, and therefore, the liquidus constants

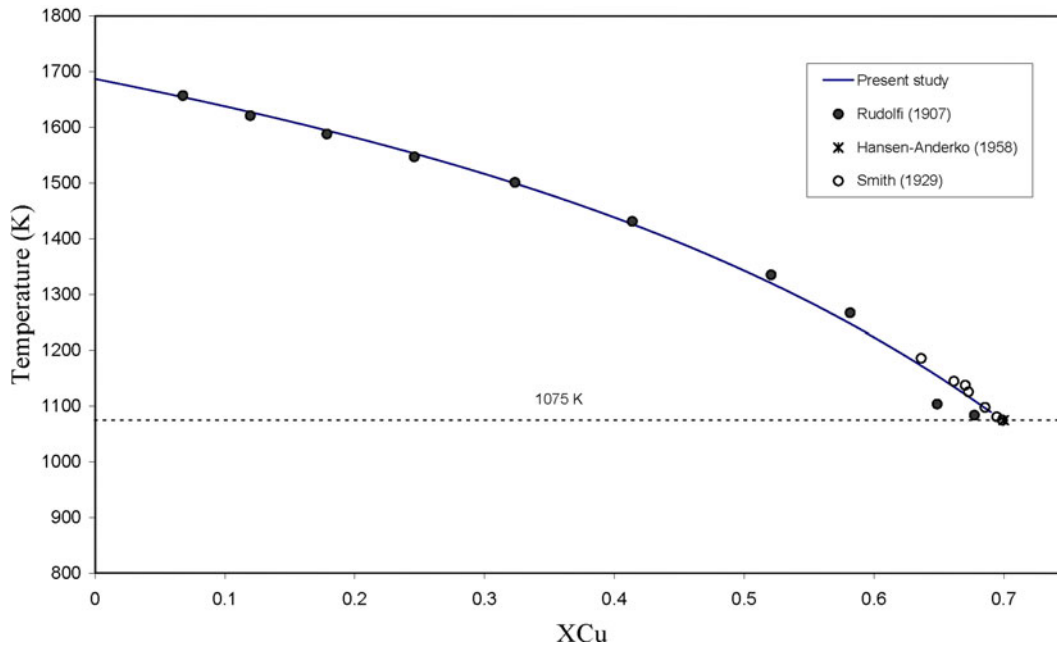


Fig. 10—The liquidus on the silicon portion of Si-Cu system.

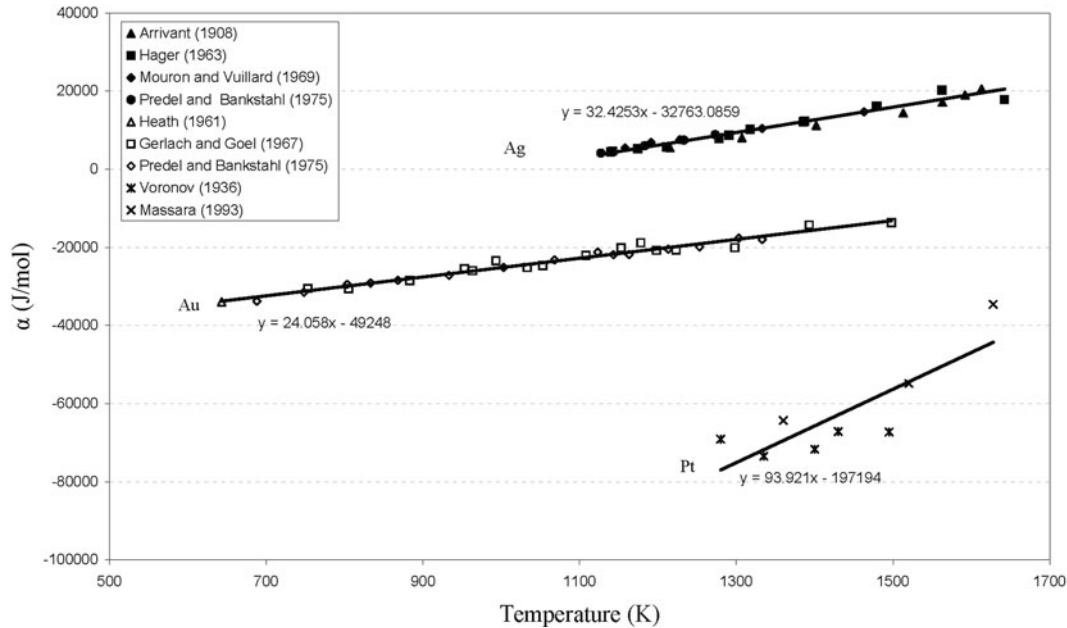


Fig. 11—The relationship between parameter α and temperature for Si-Ag, Si-Au, and Si-Pt systems.

of $a = -41,822$ J/mol and $b = -24.06$ J/mol-K are obtained. These values are different compared with the previously calculated values as $a = -49,834$ J/mol and $b = -30.08$ J/mol-K.^[4]

The calculated liquidus curve using the determined liquidus constants in this study is illustrated in Figure 10. Obviously, the calculated liquidus fits well with the liquidus measurements. This liquidus gives the composition $X_{Si} = 0.304$ at the eutectic temperature 1075 K (802 °C), which is located between the reported eutectic compositions mentioned previously.^[48]

H. Si-Ag System

The Si-Ag system is a simple eutectic, and according to the recent works the eutectic coordinates are $T = 1108$ K (835 °C) and $X_{Si} = 0.11$ ^[53] or $T = 1110.3$ K (837.2 °C) and $X_{Si} = 0.10$.^[54] The liquidus of this system has been studied by thermal analysis in several studies.^[55–58]

Considering the liquidus data of the Si-Ag system, the corresponding α -values plotted against temperature in Figure 11 are calculated. The trend line yields

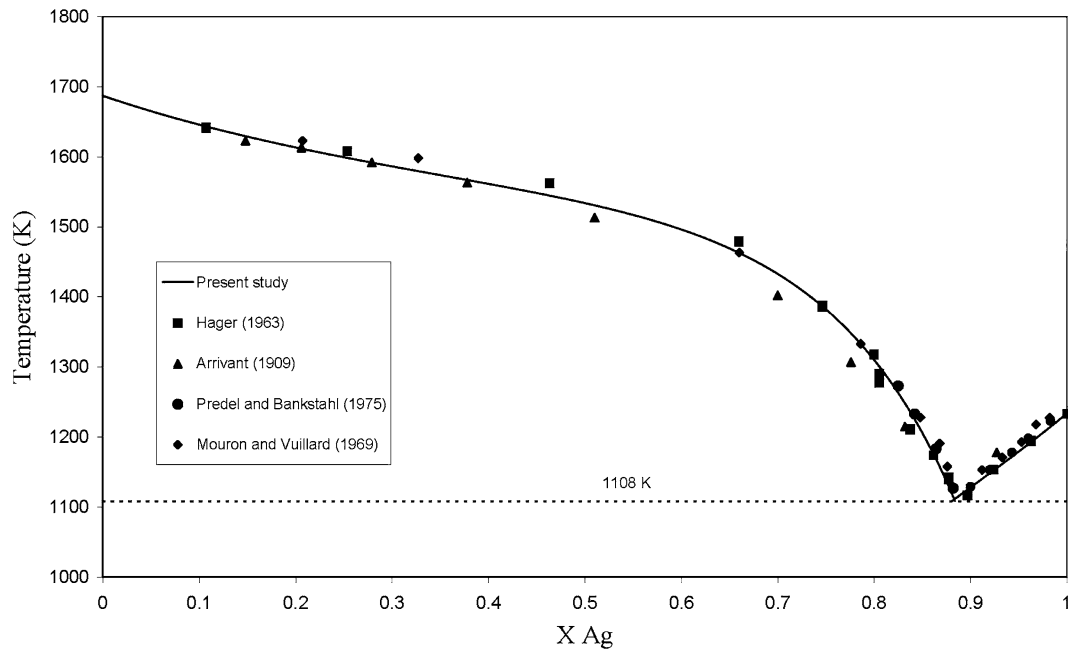


Fig. 12—The liquidus of Si-Ag system.

liquidus constants of $a = -32,763.1$ J/mol and $b = -32.43$ J/mol-K, which are close to the calculated values by Thurmond and Kowalchik ($a = -33,097$ J/mol and $b = -31.92$ J/mol-K). However, the current calculated values are based on more experimental data after their study. The liquidus curve on the silicon side of Si-Ag system has been calculated using the calculated liquidus constants by Eq. [9], and the result is shown in Figure 12 together with the experimental measurements.

Similar to the Si-Al system described previously, the hypereutectic liquidus in Si-Ag system can also be calculated. Figure 12 illustrates the consequence liquidus with considering $\Delta H_{f,Ag}^0 = 11,088.12$ J/mol and $T_{f,Al} = 1233.8$ K (960.8 °C) in an equation similar to Eq. [10] for silver. The obtained liquidus for silver portion of the phase diagram is illustrated in Figure 12, and it is correlated with the experimental data. The calculated liquidus curves cross at $X_{Si} = 0.116$ and $T = 1108$ K (835 °C), which gives the same eutectic temperature and close composition to the work done by Olesinski *et al.*[53]

I. Si-Au System

The Si-Au phase diagram has been assessed by Elliot and Shunk,[59] Chevalier,[60] and Okamoto and Massalski.[61] According to the latter work, this system contains a eutectic reaction with the eutectic coordinates $T = 633$ K (360 °C) and $X_{Si} = 0.197$. Thermal analysis was used by Di Capua[62] to establish the phase diagram and he indicated that this binary system is a eutectic system. The later studies on the system using thermal analysis[58,63,64] are more consistent and they show a eutectic point in much lower silicon concentration than what determined by Di Capua. This may be related to the significant amount of impurities (around 5 pct) in

the used silicon by Di Capua. Hence, more recent experimental data are considered to calculate the liquidus constants here for the silicon portion of the system.

Using the liquidus data reported on the silicon side of the Si-Au system, the α values, which are plotted in Figure 11 against the corresponding temperatures, are obtained. The trend line through these values gives the liquid constants of $a = -49,248$ J/mol and $b = -24.06$ J/mol-K. Thus, these liquidus constants are different with the previous calculated values as $a = -81,759.2$ J/mol and $b = -43.01$ J/mol-K by Thurmond and Kowalchik.[4] This is because they included the data from Di Capua, which are in low accuracy. Figure 13 shows the liquidus curve calculated by the determined liquidus constants in this study together with the reported experimental data. The calculated liquidus gives a eutectic composition of $X_{Si} = 0.183$ at the temperature 633 K (360 °C), which is close to the reported eutectic coordinates reported in literature, such as $X_{Si} = 0.186$ and $T = 643$ K (370 °C),[63] $X_{Si} = 0.1704$ and $T = 643$ K (370 °C),[64] and $X_{Si} = 0.186$ and $T = 636$ K (363 °C).[61]

J. Si-Pt System

The equilibrium binary system of Si-Pt has been assessed recently by Xu *et al.*[65] This phase diagram has a eutectic reaction on the silicon side with the coordinates of 1220 K (947 °C) and $X_{Si} = 0.654$. The liquidus in this system was first measured by Voronov[66] in 1936 using thermal analysis. This phase diagram was also studied by Massara and Feschotte[67] using DTA, X-ray diffraction, and microprobe analysis. The liquidus measurements on the silicon-rich part of the phase diagram in these studies are consistent.

Using the experimental data to calculate α values and plotting them against the corresponding temperatures gives the liquidus constants $a = -197,194 \text{ J/mol}$ and $b = -93.921 \text{ J/mol-K}$ (Figure 11). These data were used to calculate the liquidus on the silicon portion of the phase diagram, which is shown in Figure 14. The calculated liquidus curve gives $X_{\text{Si}} = 0.6564$ at $T = 1220 \text{ K}$ ($947 \text{ }^\circ\text{C}$), which is close to the calculated eutectic point by Xu *et al.*^[65]

K. Si-Sn System

The Si-Sn system contains a eutectic that lies close to the tin side. This point has been calculated to be at $X_{\text{Si}} = 1 \times 10^{-7}$ and $T = 505 \text{ K}$ ($232 \text{ }^\circ\text{C}$),^[4] $X_{\text{Si}} = 5 \times 10^{-7}$ and $T = 504.9 \text{ K}$ ($231.9 \text{ }^\circ\text{C}$),^[68] and $X_{\text{Si}} = 4 \times 10^{-7}$ and $T = 505.08 \text{ K}$ ($232.08 \text{ }^\circ\text{C}$).^[69] The liquidus in this system has been determined by thermal analysis,^[70] using crystal pulling and thermal gradient

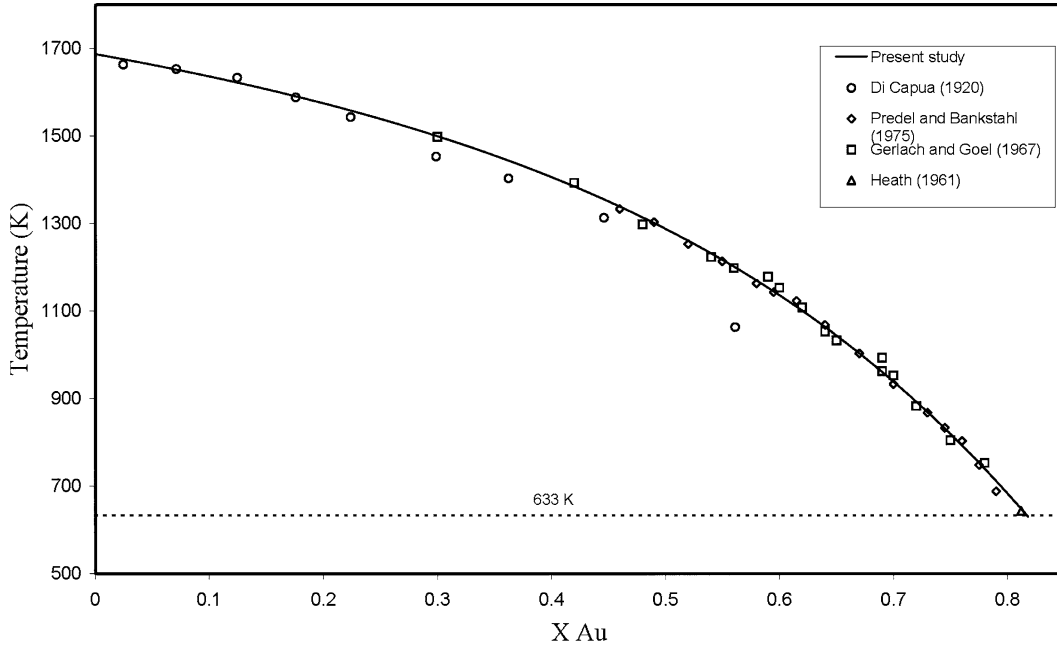


Fig. 13—The liquidus on the silicon portion of Si-Au system.

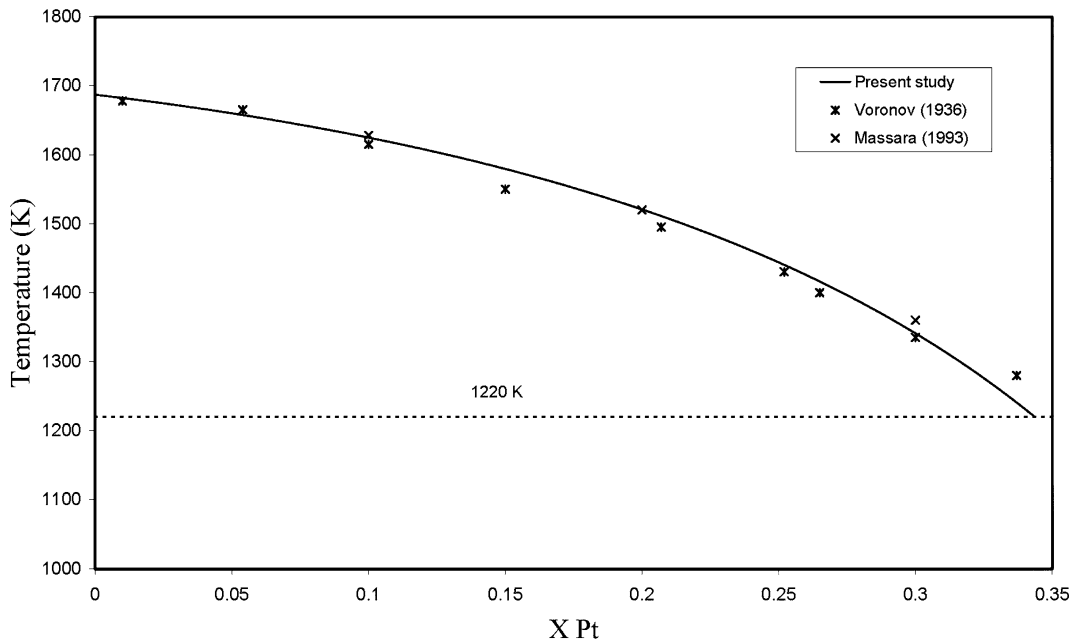


Fig. 14—The liquidus on the silicon portion of Si-Pt system.

techniques,^[71] the gravimetric method,^[4] and DTA.^[72] The so far measured liquidus data by Tamaru^[70] are not considered in the calculations here because of the existence of significant iron impurity (7.5 wt pct) in their original silicon.

The plot of the calculated parameter α against temperature for the measured experimental data^[4,16,71,72] is shown in Figure 15. The trend line gives the liquidus constants equal to $a = 31,162$ J/mol and $b = 4.03$ J/mol-K, which are relatively close to the former calculations by Thurmond and Kowalchik ($a = 34,080$ J/mol and $b = 6.28$ J/mol-K). The calculated liquidus for the Si-Sn system by the obtained liquidus constants is shown in Figure 16 together with the experimental measurements. As is shown, the reported experimental data at high temperatures by Kobylkin *et al.*,^[72] which were not used for the liquidus constant calculations, can be predicted fairly by the calculated liquidus. The calculated liquidus gives a eutectic composition at $X_{Si} = 2 \times 10^{-7}$ at 505 K (232 °C), which is in the range of the previously mentioned coordinates for the liquidus.

L. Si-Pb System

The phase diagram of Si-Pb is dominated by a miscibility gap in the liquid phase that extends from 1675 K (1402 °C) up to high temperatures, probably in excess of 2300 K (2027 °C). Experimental measurements, however, have been carried out only over a limited temperature range. Olesinski and Abbaschian^[73] calculated the phase boundaries, assuming a pseudo regularity of the system, and according to them, there is a monotectic reaction on the silicon side at 1675 K (1402 °C)

and $X_{Si} = 0.975$. At this point, a silicon-rich melt is transformed to solid silicon and a dilute solution of Si in liquid Pb. There is a eutectic at low temperatures in this system where liquid is transformed to Si and Pb. The coordinates of this eutectic have been calculated as $X_{Si} = 9 \times 10^{-10}$ at 600 K (327 °C).^[49]

The solubility of silicon in molten lead has been measured by Moissan and Siemens^[44] and Thurmond and Kowalchik^[4] using a gravimetric technique. Applying the liquidus measurements, as was done recently for the Si-Pb system,^[4] the α - T plot shown in Figure 14 is obtained. The trend line yields $a = 79,639$ J/mol and $b = 17.08$ J/mol-K, which were calculated previously using the same experimental data.^[4] The calculated liquidus using these constants (Figure 17) predicts a monotectic reaction at 1675 K (1402 °C) at $X_{Si} = 0.972$, which is close to the reported monotectic point by Olesinski and Abbaschian.^[73] Moreover, the solubility of silicon in lead at the monotectic reaction is calculated as $X_{Si} = 0.028$. The calculated liquidus for the Pb side gives a eutectic composition of $X_{Si} = 1.3 \times 10^{-9}$ at 600 K (327 °C).

M. Si-Bi System

Similar to the Si-Pb system, the binary phase diagram of Si-Bi system contains a monotectic reaction, which is at 1673 K (1400 °C) and $X_{Si} = 0.967$ according to the assessed phase diagram by Olesinski *et al.*^[74] In this system a eutectic point exist on the Bi portion at $X_{Si} = 1 \times 10^{-10}$ and 544 K (271 °C). The liquidus in the area between the eutectic and the monotectic temperatures was measured by Williams in 1907,^[75] Thurmond and Kowalchik in 1960,^[4] and Girault *et al.* in 1977.^[16] The measurements done by Williams are not

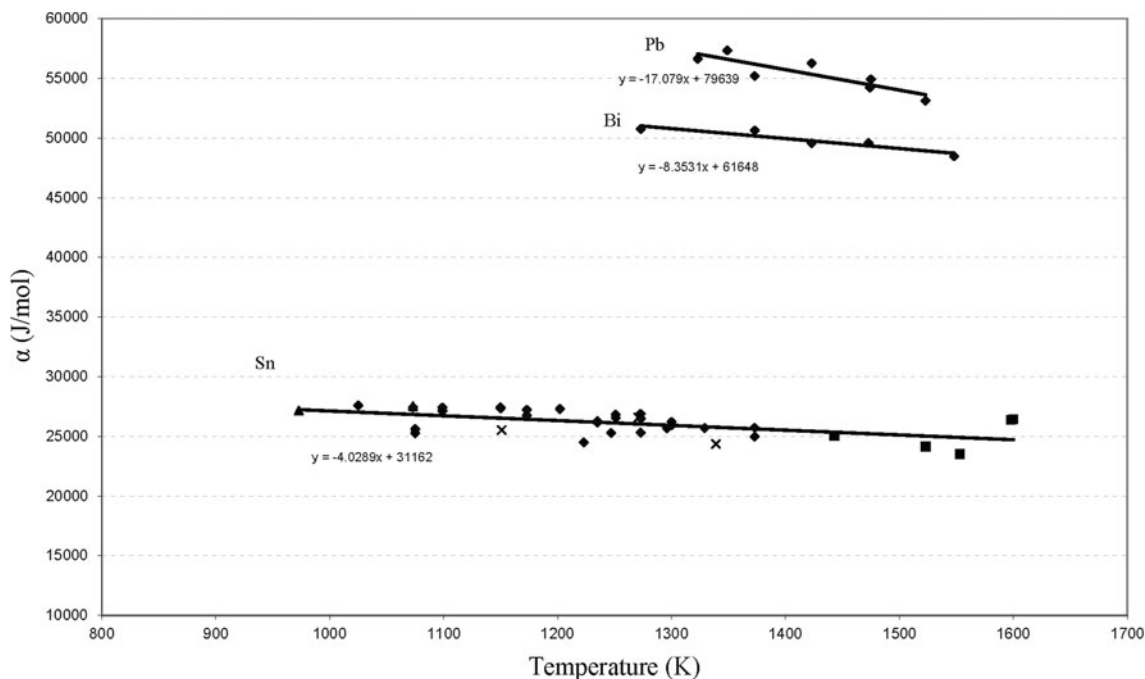


Fig. 15—The relationship between parameter α and temperature for Si-Sn, Si-Pb, and Si-Bi systems.

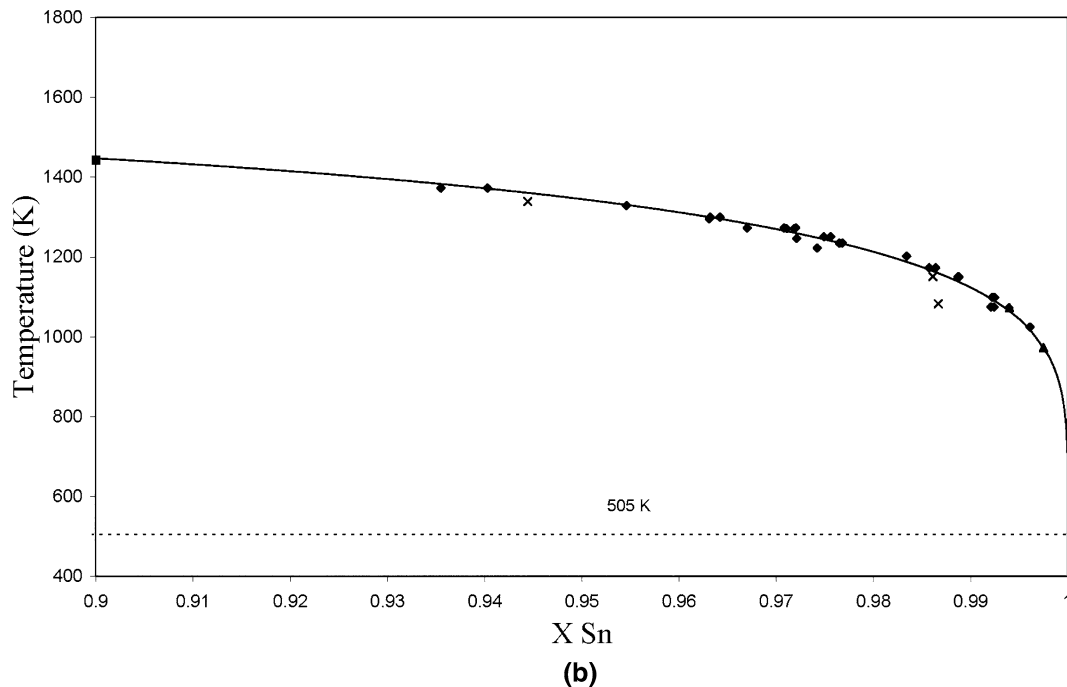
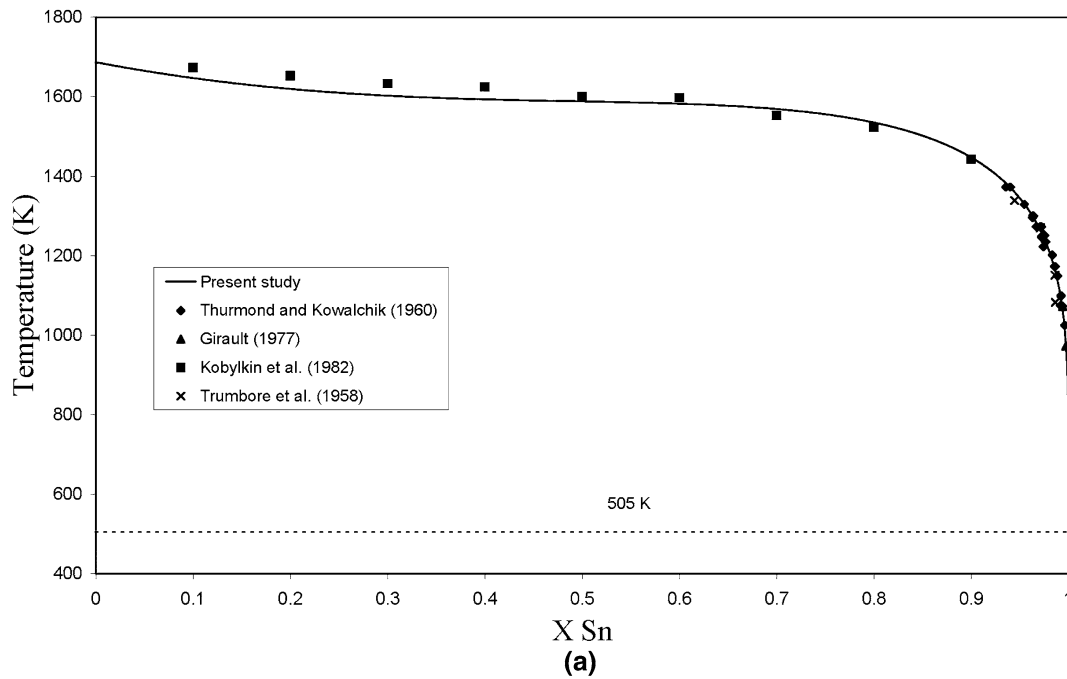


Fig. 16—The liquidus of Si-Sn system.

accurate because approximately 2 pct impurities (Al and Fe) existed in the sample.

The calculated α from the point reported by Girault can be considered as an outlier compared with the other calculated values from the experimental data.^[4] Thus, plotting α - T variations with using the consistent data,^[4] the liquidus constants are calculated as $a = 61,648$ J/mol and $b = 8.35$ J/mol-K. The calculated liquidus using these values indicates a monotectic reaction at 1673 K (1400 °C) at $X_{Si} = 0.967$ (Figure 18). In addition, the solubility of silicon in

molten bismuth at the monotectic temperature is obtained as $X_{Si} = 0.038$. The calculated liquidus gives the eutectic composition as $X_{Si} = 1.7 \times 10^{-9}$ at 544 K (271 °C).

N. Si-Sb System

The binary Si-Sb system was assessed by Olesinski and Abbaschian^[76] using the experimental data reported in other studies.^[4,16,75,77] According to them, this system has a eutectic transformation at 902.7 K (629.7 °C)

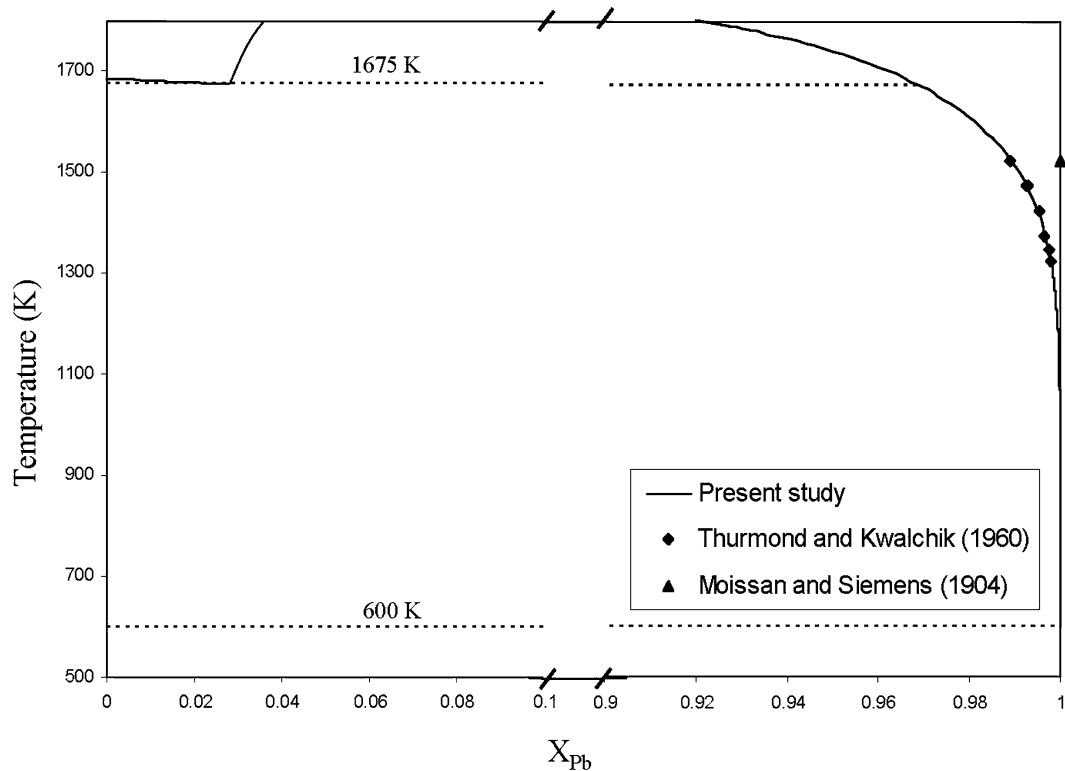


Fig. 17—The liquidus on Si and Pb portions of Si-Pb system.

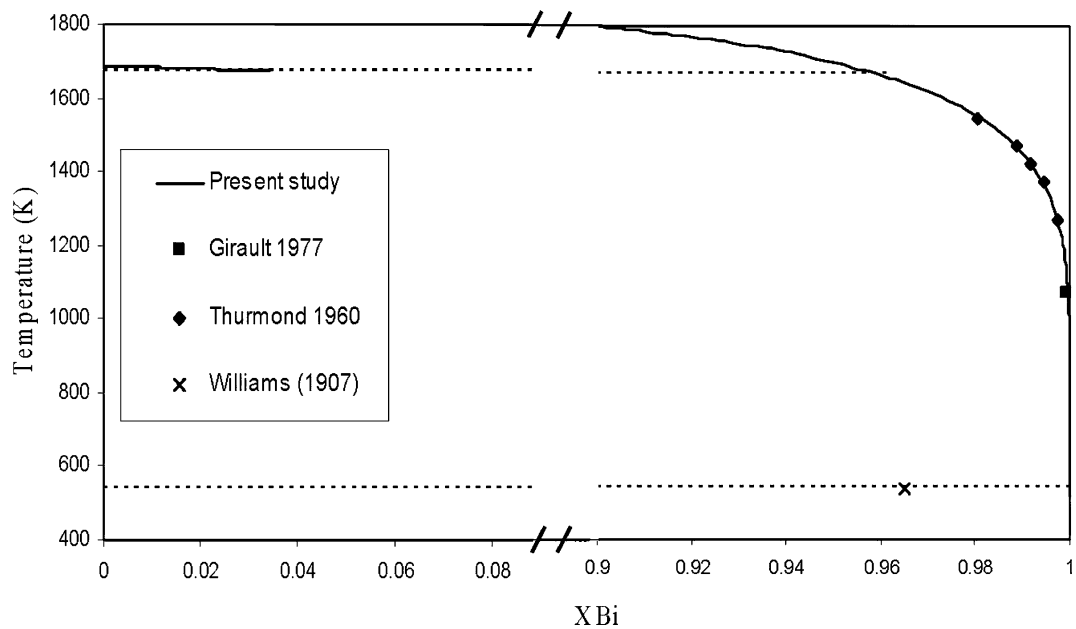


Fig. 18—The liquidus on Si and Bi portions of Si-Bi system.

and $X_{Si} = 0.003$. The measured data so far by Williams^[75] are not accurate because of the existence of considerable impurities in the used silicon.^[75] Calculating parameter α from other studies, the liquidus constants $a = 14,273$ J/mol and $b = -5.99$ J/mol-K are obtained (Figure 19). These values are relatively close to

the calculations done by Thurmond and Kowalchik as $a = 13,766$ J/mol and $b = -6.74$ J/mol-K,^[4] and Olesinski and Abbaschian as $a = 16,297$ J/mol and $b = -3.91$ J/mol-K.

The calculated liquidus curve presented in Figure 20 fits well with the experimental measurements. The

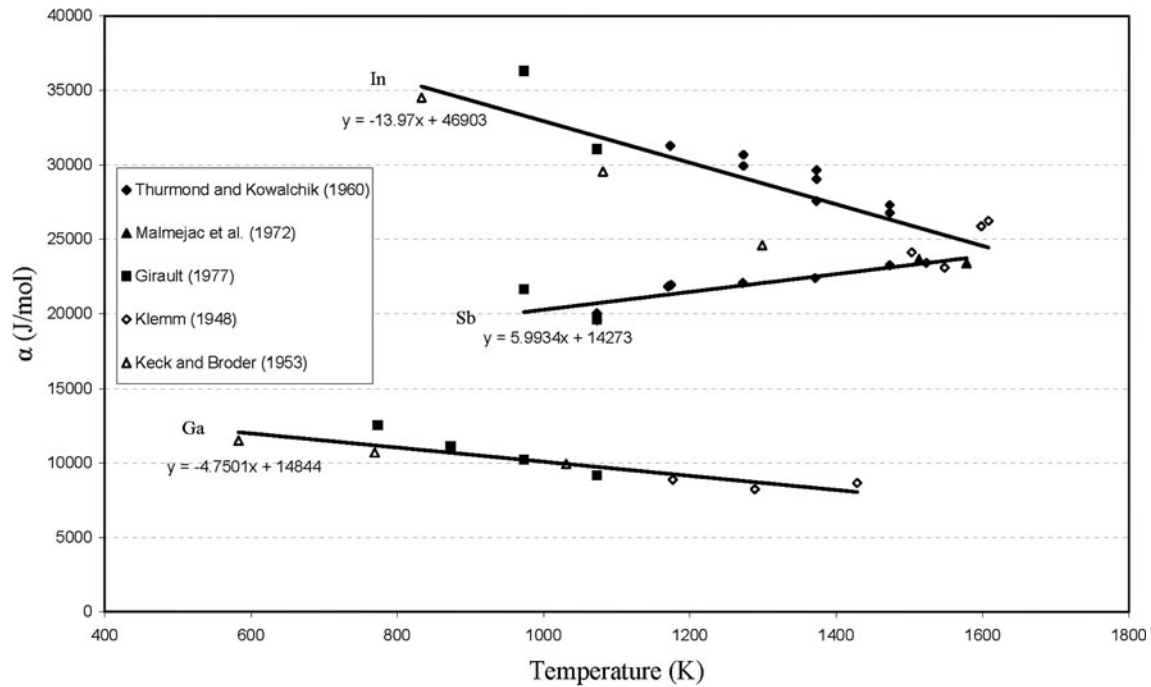


Fig. 19—The relationship between parameter α and temperature for Si-Sb, Si-Ga, and Si-In systems.

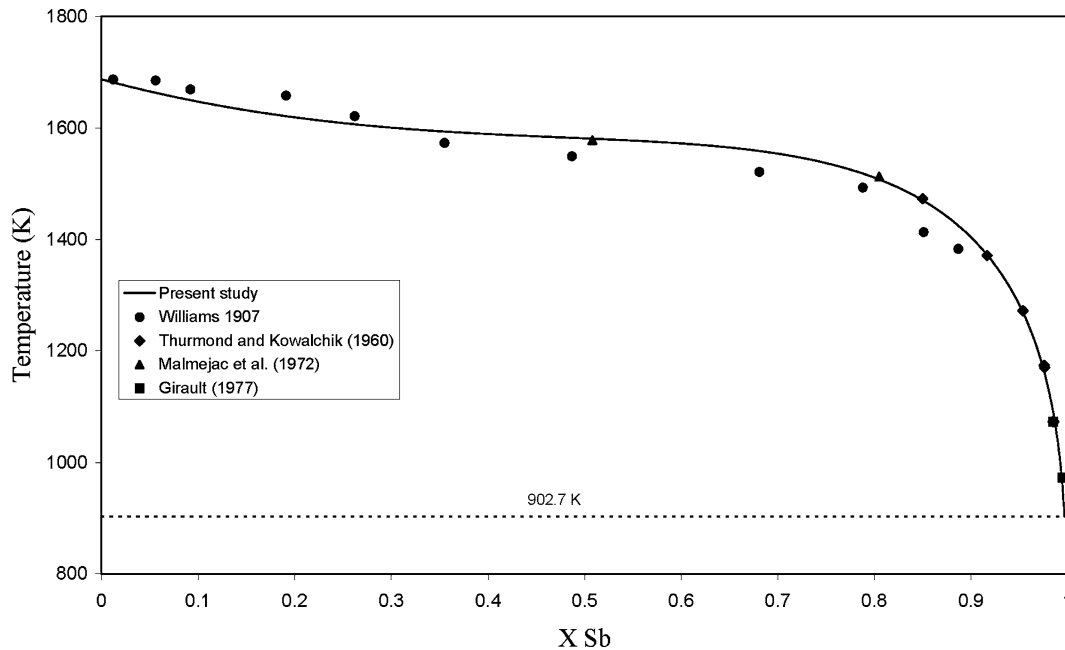


Fig. 20—The liquidus of Si-Sb system.

calculated liquidus suggests that at the eutectic temperature of 902.7 K (629.7 °C), the composition is $X_{\text{Si}} = 0.0032$, which is close to the above reported composition.

O. Si-Ga System

According to the assessed Si-Ga phase diagram by Olesinski *et al.*,^[78] a eutectic transformation exists in

this system at 302.77 K (29.77 °C). The liquidus in this system has been measured through thermal analysis,^[79] weighing technique,^[14,80] thermal analysis, and metallography.^[81] The latter liquidus data seems not to be accurate and they are relatively lower than in other works. Using the liquidus measurements of the three former studies led to the illustrated α - T plot in Figure 19 which gives the liquidus constants $a = 14,844$ J/mol and $b = 4.75$ J/mol-K. These values are close to the

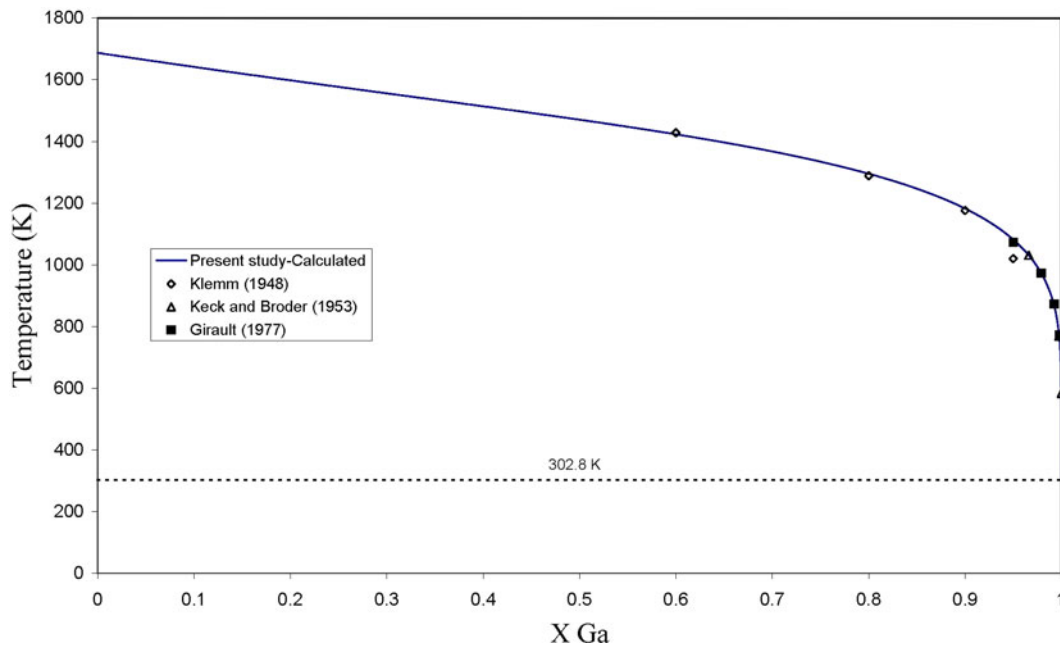


Fig. 21—The liquidus of Si-Ga system.

reported data by Thurmond and Kowalchik as $a = 13,599$ J/mol and $b = 3.74$ J/mol-K,^[4] and by Olesinski *et al.*^[78] as $a = 14,900$ J/mol and $b = 4.90$ J/mol-K.

The calculated liquidus curve using the obtained liquidus constants is shown in Figure 21. The calculations show a eutectic composition at the eutectic temperature as $X_{\text{Si}} = 3 \times 10^{-10}$, which is close to the mentioned eutectic compositions as $X_{\text{Si}} = 5 \times 10^{-10}$ ^[4] and $X_{\text{Si}} = 6 \times 10^{-10}$.^[78]

P. Si-In System

The equilibrium Si-In phase diagram was assessed by Olesinski *et al.*,^[82] and it is a simple eutectic system where the eutectic reaction takes place at 429.63 K (156.63 °C) on the indium portion. This phase diagram has been based on liquidus determinations through a thermal analysis^[79] and weighting techniques.^[4,16,80]

Calculating α values from the reported liquidus data with Eq. [8] and drawing them against the corresponding temperatures (Figure 19) yields the liquidus constants $a = 46,903$ J/mol and $b = 13.97$ J/mol-K. These values are close to the calculated values by Thurmond and Kowalchik as $a = 47,909$ J/mol and $b = 14.1$ J/mol-K and those calculated by Olesinski *et al.* as $a = 45,100$ J/mol and $b = 12.8$ J/mol-K. The calculated liquidus curve using the determined liquidus constants by Eq. [9] is shown in Figure 22, and as shown in the calculated curve, it can explain the liquidus in the whole composition range. Similar to the Si-Ga system, the current calculated liquidus suggests that the eutectic composition is in low silicon concentration $X_{\text{Si}} = 2.5 \times 10^{-10}$, which is close to the previously calculated eutectic composition as $X_{\text{Si}} = 2 \times 10^{-10}$.^[4]

Q. Si-Pd System

The thermodynamics of Si-Pd system has been studied recently by Okamoto^[83] and Du *et al.*^[84] This system has a eutectic reaction on the silicon side at 1165 K (892 °C) and $X_{\text{Si}} = 0.52$ ^[85,86] or 1138 K (865 °C) and $X_{\text{Si}} = 0.518$.^[83] The liquidus between this point and silicon has been measured experimentally.^[85–88] The few liquidus measurements done by Rao and Winterhager^[87] are not consistent compared with the measurements done using DTA, magnetic thermal analysis, and metallographic analysis,^[85] and those done by using DTA.^[86] The measured liquidus data by Tsumori and Akimune^[88] are not reliable because of the application of high cooling rates in their thermal analysis experiments and thus obtaining much lower liquidus temperature than other experimental works.

Considering the reliable liquidus data,^[85,86] the α - T plot shown in Figure 23 for silicon-rich Si-Pd alloys is obtained. The trend line gives the liquidus constants of $a = -73,424$ J/mol and $b = -28.385$ J/mol-K. These values lead to the calculated liquidus, which is shown in Figure 24. This liquidus curve gives $X_{\text{Si}} = 0.52$ and $X_{\text{Si}} = 0.504$ at the proposed eutectic temperatures 1165 K (892 °C) and at 1138 K (865 °C), respectively. The former coordinate is the same as the reported eutectic coordinates,^[85,86] whereas the latter coordinate is a little in lower silicon concentration than what suggested for the eutectic recently.^[84]

R. Si-Ni System

The silicon portion of equilibrium Si-Ni system was established by Iwase and Okamoto.^[89] The whole phase diagram was later evaluated extensively.^[90] The thermodynamics of this system has been also studied in

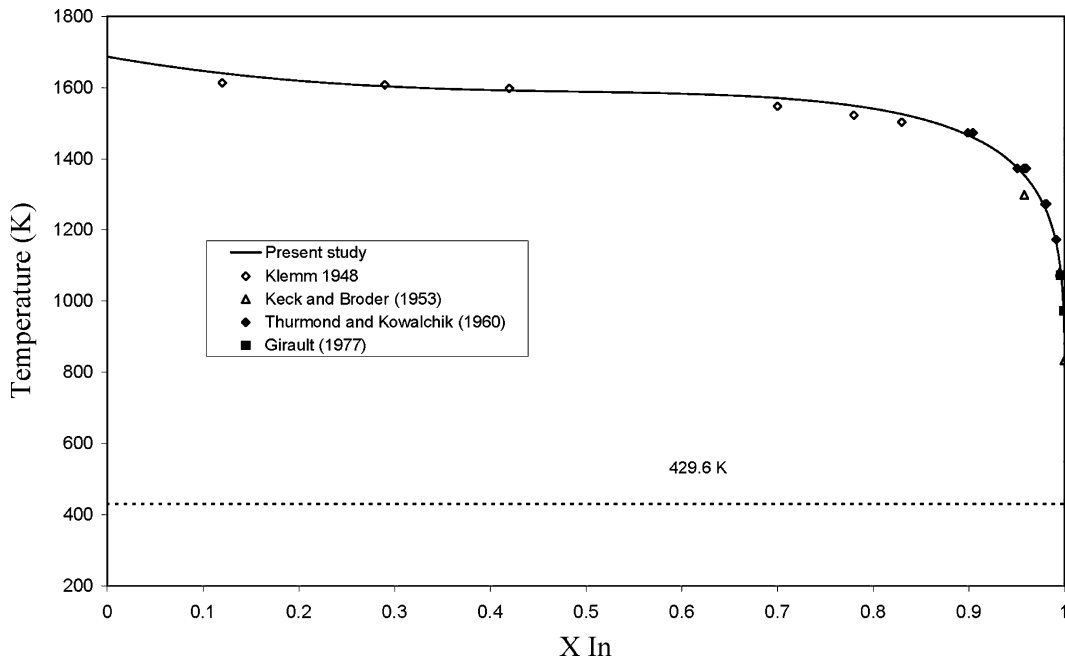


Fig. 22—The liquidus of Si-In system.

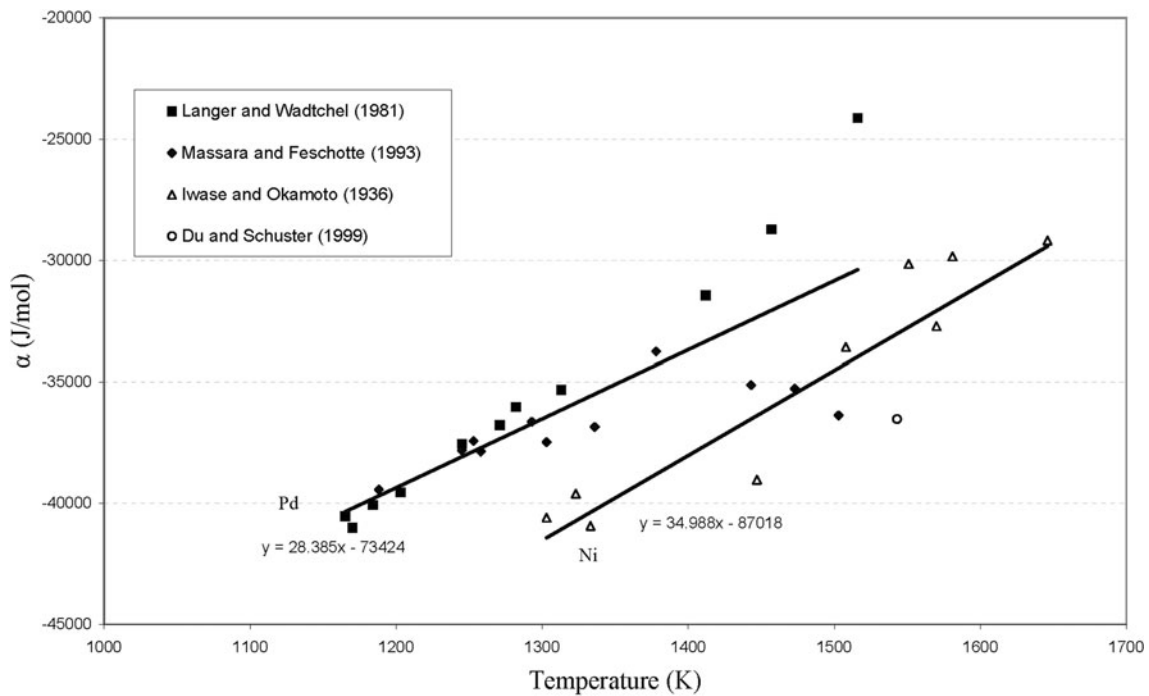


Fig. 23—The relationship between parameter α and temperature for Si-Pd and Si-Ni systems.

other works.^[91,92] In this system, the nickel silicides NiSi and NiSi₂ are the two existing stoichiometric intermediate compounds. On the silicon side of the phase diagram, a peritectic reaction takes place, where solid NiSi₂ is formed through the interaction of solid silicon and a liquid phase. This transformation takes place at 1266 K (993 °C)^[89–91] or 1243 K (970 °C).^[92] The liquid phase in the peritectic reaction contains 59 at. pct Si^[89,90] or 60.1 at. pct Si.^[91] The liquidus at higher

silicon concentrations than this has been measured by Iwase and Okamoto^[89] and Du and Schuster.^[92]

The calculated a values against the corresponding temperatures of the liquidus measurements of high silicon Si-Ni alloys are plotted in Figure 23. The related trend line gives the liquidus constants $a = -87,018$ J/mol and $b = -34.99$ J/mol-K. The calculated liquidus with using these constants is shown in Figure 25 with the experimental data in this region. The obtained curve predicts a

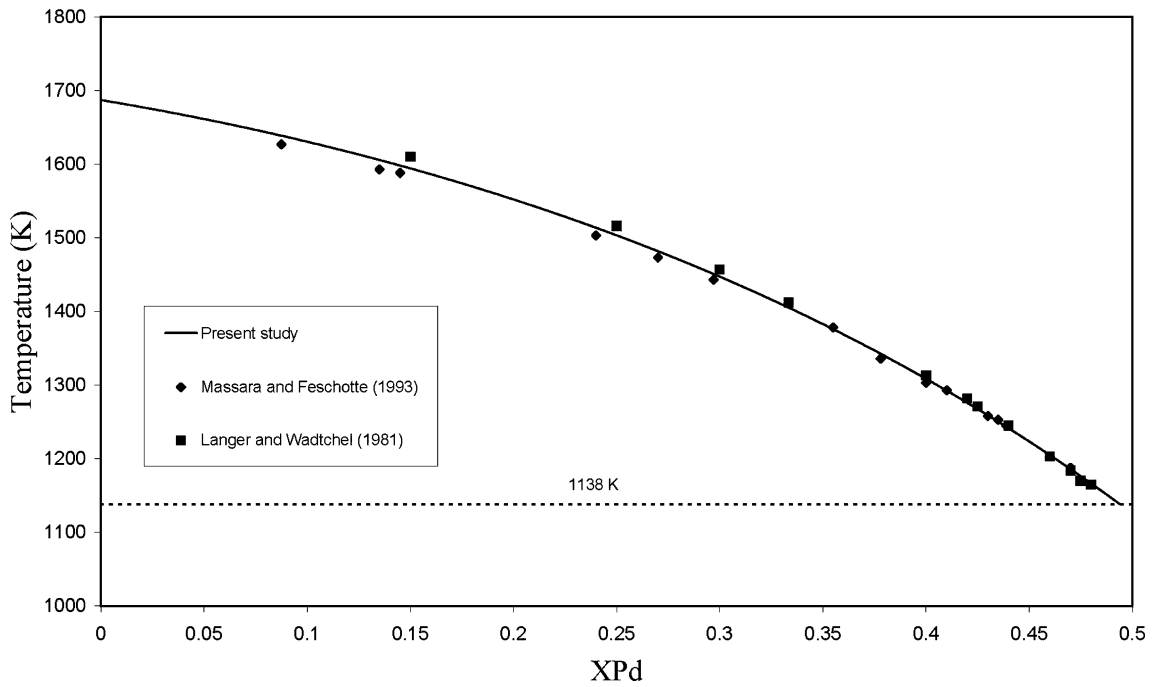


Fig. 24—The liquidus on the silicon portion of Si-Pd system.

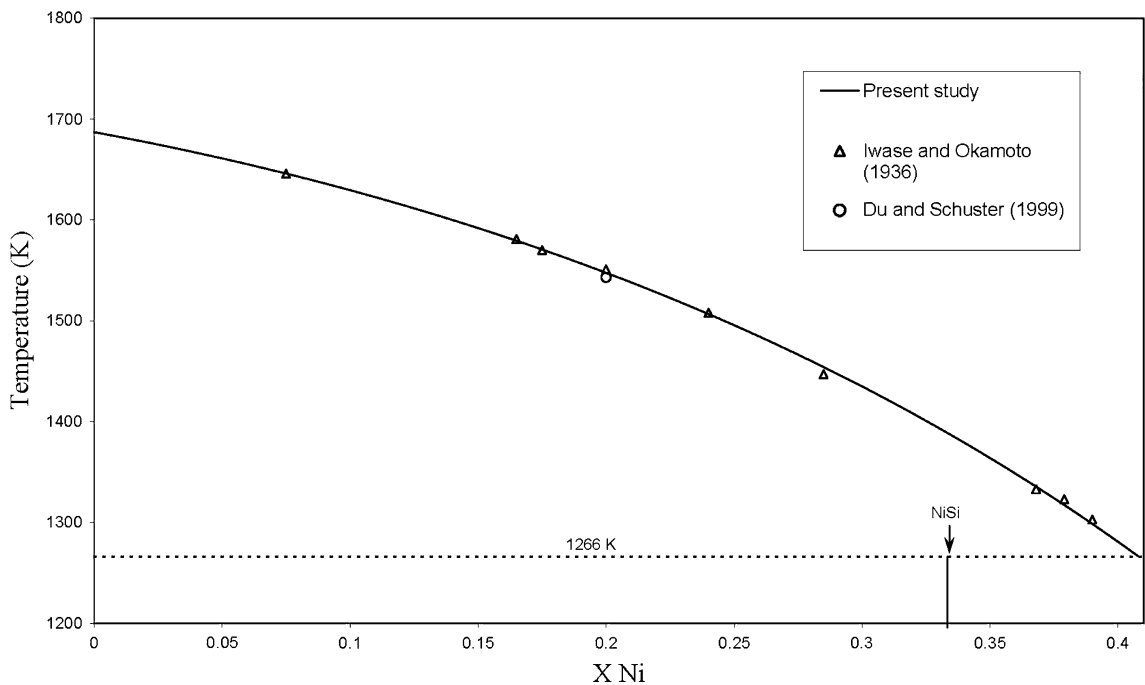


Fig. 25—The liquidus on the silicon portion of Si-Ni system.

liquid composition in equilibrium with Si and NiSi₂ at 1266 K (993 °C) with $X_{Si} = 0.591$, which is very close to the literature data.

S. Si-Mn System

So far, the liquidus of the whole Si-Mn binary system was studied by Doerinkel.^[93] The liquidus on the Si side

was also measured by Dudkin and Koznetsova,^[94] Morokhovets *et al.*,^[95] and Mager and Wachtel.^[96] The thermodynamics of this system has also been studied in several studies.^[43,98–101] In this system, a eutectic point exists on the silicon-rich part where a liquid with 66.4 at. pct Si is in equilibrium with solids of silicon and Mn₁₉Si₁₁ at 1423.2 K (1150.2 °C).^[98] Close eutectic coordinates as $X_{Si} = 0.679$, $T = 1423.15$ K

(1150.15 °C)^[96] and $X_{Si} = 0.6708$, $T = 1419.7$ K (1146.7 °C)^[101] has also been reported.

Inspecting the liquidus measurements for higher silicon concentrations than the above eutectic point, it is found that the measurements done by Doerinkel^[96] are low in accuracy because they measured the silicon melting point more than 40° higher than the pure silicon melting point. The liquidus measurements done by Fujino *et al.*^[97] are also relatively lower than other reported liquidus data

and might be in low accuracy. Considering the measurements done in other works,^[94-96] the α - T plot shown for Mn in Figure 26 is obtained. The trend line gives liquidus constants $a = -12,344$ J/mol and $b = -64.86$ J/mol-K. The illustrated liquidus curve in Figure 27 is calculated using these constants, and it predicts a eutectic composition as $X_{Si} = 0.67$ at 1415 K (1142 °C), which is close to the previously mentioned coordinates for the eutectic point.

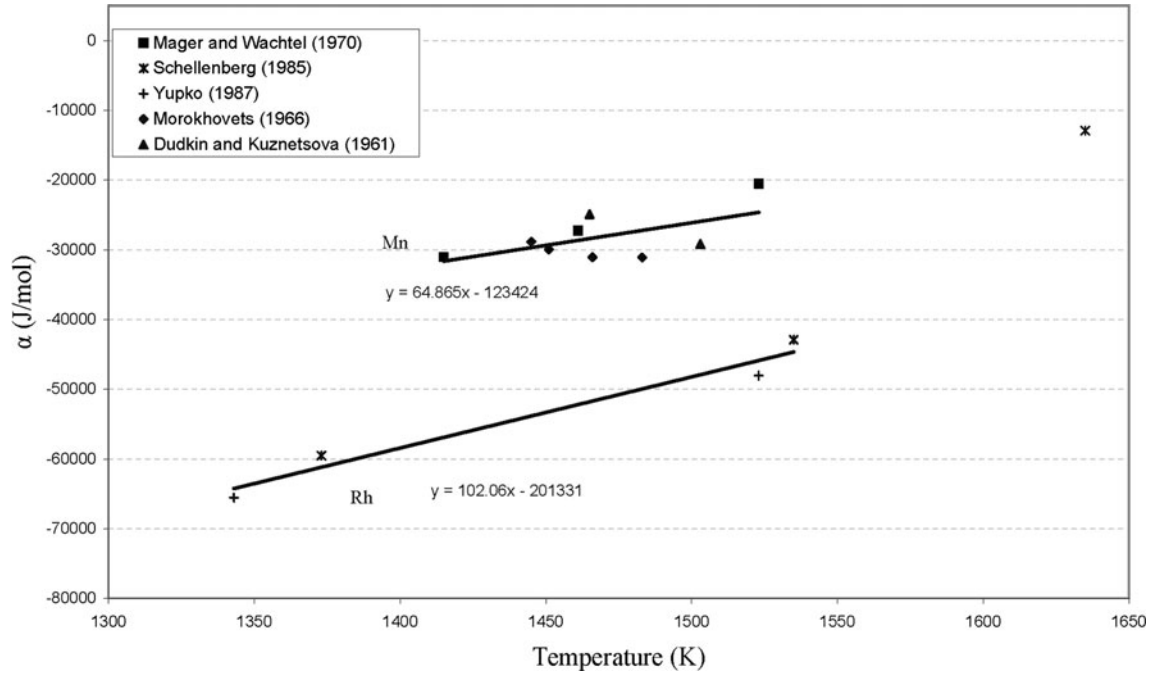


Fig. 26—The relationship between parameter α and temperature for Si-Mn and Si-Rh systems.

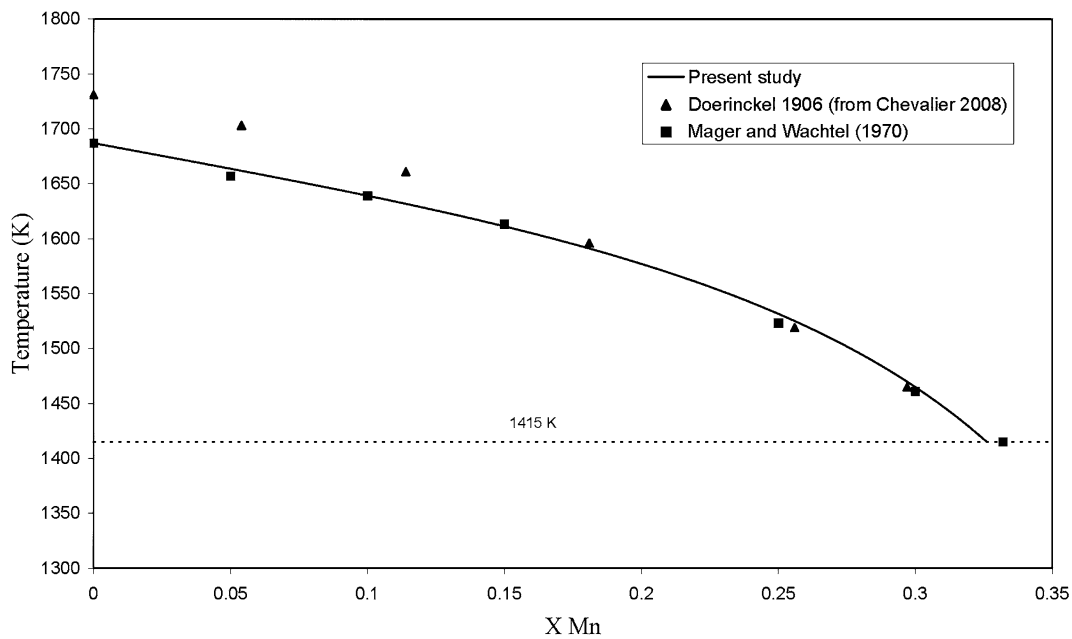


Fig. 27—The liquidus on the silicon portion of Si-Mn system.

T. Si-Rh System

Schellenberg *et al.*^[102] investigated the Si-Rh phase diagram by means of X-ray powder diffraction, DTA, metallography, and electrical resistivity measurements. Some parts of this system were later studied by Yupko.^[103] Moreover, the assessment of this system was carried out by Schlesinger.^[104] A eutectic reaction takes place on the silicon side at $X_{\text{Si}} = 0.685$ and $T = 1333 \text{ K}$ (1060 °C),^[102,104] where a liquid is transformed to solid silicon and rhodium silicide Rh_3Si_4 .

Figure 26 shows the calculated α values against temperature using the liquidus measurements at higher silicon concentrations than the previously mentioned eutectic point. This plot yields the liquidus constants $a = -201,331 \text{ J/mol}$ and $b = -102.06 \text{ J/mol-K}$. The calculated liquidus by these constants is illustrated in Figure 28 and it fits well with the experimental measurements. This liquidus predicts a eutectic at $X_{\text{Si}} = 0.686$ at 1333 K (1060 °C), which is close to the mentioned eutectic composition in literature.

IV. EVALUATION OF THE LIQUIDUS CONSTANTS

The determined liquidus constants and the calculated eutectic points in the current study are summarized in Table II. These results can be used to study the behavior of the silicon melts as discussed in the following.

A. The Behavior of Silicon Solutions

Considering the a and b values in Table II, it is observed that for most silicon binary systems, except Si-Al and Si-Sb, both a and b have the same sign—negative or positive. Because there is a direct relation between the parameter a and the changes in the relative

partial molar heat of solution components according to Eq. [6], the total enthalpy of mixing have the same sign as parameter a . Hence, the change in the solution enthalpy of mixing is negative for negative a values and it is positive for positive a values. From a thermodynamics point of view, a negative enthalpy of mixing or, here, negative a value indicate negative deviation from the Raoult's law, and vice versa.^[2] Therefore, we may conclude that silicon binary solutions with Al, Ca, Mg, Fe, Ti, Cu, Ag, Au, Pt, Pd, Ni, Mn, and Rh have

Table II. The Calculated Liquidus Constants and Eutectic Compositions for Silicon Binary Systems

System	a	b	$T_{\text{eut. K}} (\text{°C})^*$	$X_{\text{Si,eut.}}$
Si-Al	-9789.7	3.7402	850.1 (577.1)	0.119
Si-Ca	-83,820	-0.2271	1296 (1023)	0.694
Si-Mg	-73,857	-32.612	1217 (944)	0.527
Si-Fe	-99,915	-47.18	1479 (1206)	0.724
Si-Ti	-328,815	-167.32	1591 (1318)	0.87
Si-Zn	29,206	16.26	692.2 (419.2)	2.5×10^{-4}
Si-Cu	-41,822	-24.056	1075 (802)	0.304
Si-Ag	-32,763.1	-32.42	1108 (835)	0.116
Si-Au	-49,248	-24.058	633 (360)	0.183
Si-Pt	-197,194	-93.921	1220 (947)	0.656
Si-Sn	31,162	4.0289	505 (232)	2×10^{-7}
Si-Pb	79,639	17.079	600 (327)	$1.3 \times 10^{-9\dagger}$
Si-Bi	61,648	8.3531	544 (271)	$1.7 \times 10^{-9\dagger}$
Si-Sb	14,273	-5.99	902.7 (629.7)	3.2×10^{-3}
Si-Ga	14,844	4.75	302.8 (29.8)	3×10^{-10}
Si-In	46,903	13.97	429.6 (156.6)	2.5×10^{-10}
Si-Pd	-73,424	-28.385	1165 (892)	0.52
Si-Ni	-89,383	-36.856	1266 (993)	0.591 [‡]
Si-Mn	-12,344	-64.86	1415 (1142)	0.674
Si-Rh	-201,331	-102.06	1333 (1060)	0.686

*From the literature.

[†]Monotectic.

[‡]Peritectic.

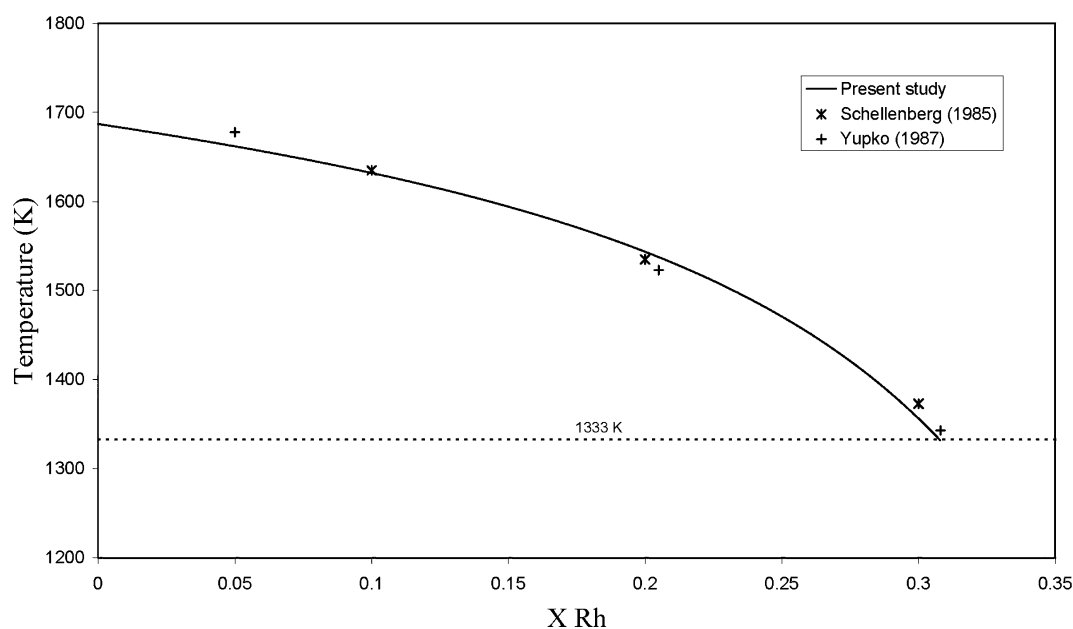


Fig. 28—The liquidus on the silicon portion of Si-Rh system.

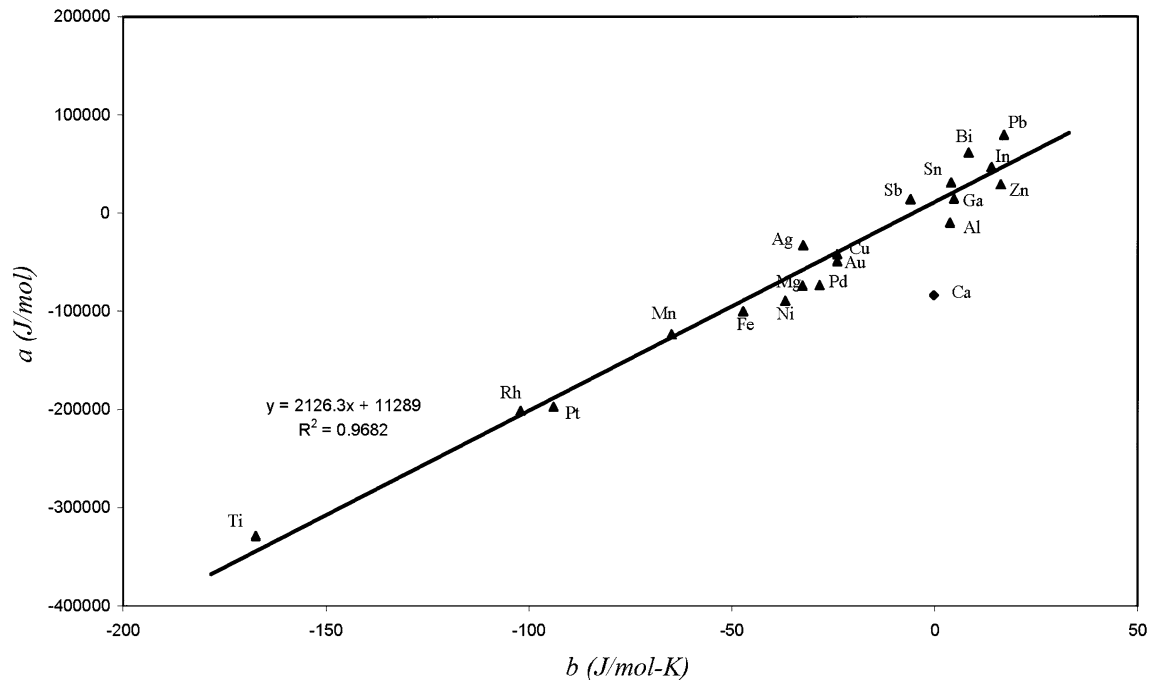


Fig. 29—The relationship between liquidus constants a and b for silicon binary systems.

negative deviation from the Raoult's law, whereas the other binary systems listed in Table II have positive deviation. This will be evaluated further in a future publication.

B. Correlation Between the Liquidus Constants

Considering Table II data, a proper correlation between the magnitude of a and b values is observed, with an exception for the Si-Ca system. A plot of the determined a values against b values for various silicon binary melts is shown in Figure 29. There is a good correlation between the two parameters with a linear relationship as:

$$a = 2126.3b + 11,289 \quad [11]$$

The existence of a linear relationship between a and b values, and so between the heat of solution and the excess entropy of solution with regard to Eqs. [6] and [7], is important and beneficial. For instance, this correlation may help us to calculate the liquidus of other silicon binary systems, which were not considered in this study. In this case, a liquidus measurement between the liquidus and the pure silicon can be used to determine the corresponding α value. Hence, considering the right-hand side of Eq. [8] and Eq. [11], we face two equations with two unknowns, and their solution yields the a and b constant for the silicon portion of the binary system.

V. CONCLUSIONS

The liquidus of 20 silicon binary systems was calculated considering the reported liquidus experimental data. For each binary system, two liquidus constants

were determined, and it was indicated that the liquidus can be calculated properly using these constants. This was shown by comparing the calculation results with the experimental data graphically. The most important contribution of the current study is introducing two constants for every silicon binary system, which can be used easily to calculate the thermodynamics properties of silicon binary melts independent from complicated thermodynamic software. It was also found that there is a linear relationship between the liquidus constants, which is useful to predict the liquidus on the silicon portion of other binary melts.

ACKNOWLEDGMENT

The authors acknowledge the project fund provided by the Norwegian Research Council through the BASIC project.

OPEN ACCESS

This article is distributed under the terms of the Creative Commons Attribution Noncommercial License which permits any noncommercial use, distribution, and reproduction in any medium, provided the original author(s) and source are credited.

REFERENCES

1. J. Schei, K. Tuset, and H. Tveit: *Production of High Silicon Alloys*, Tapir Forlag, Trondheim, Norway, 1998, pp. 17–20.

2. D.R. Gaskell: *Introduction to the Thermodynamics of Materials*, 5th ed., Taylor & Francis Group, New York, NY, 2008.
3. O. Kubaschewski and C.B. Alcock: *Metallurgical Thermo-Chemistry*, 5th ed., Pergamon Press, Oxford, UK, 1979.
4. C.D. Thurmond and M. Kowalchik: *Bell Syst. Tech. J.*, 1960, vol. 39, pp. 169–204.
5. J.L. Murray and A.J. McAlister: *Bull. Alloy Phase Diagr.*, 1984, vol. 5, pp. 74–84.
6. W. Fraenkel: *Z. Anorg. Chem.*, 1908, vol. 58, pp. 154–58.
7. C.E. Roberts: *J. Chem. Soc.*, 1914, vol. 105, pp. 1383–86.
8. A.G.C. Gwyer and H.W.L. Philips: *J. Inst. Met.*, 1927, vol. 38, pp. 31–35.
9. W. Broniewski and M. Smialowski: *Rev. Met.*, 1932, vol. 29, pp. 542–52.
10. K. Matsuyama: *Kinzoku No Kenkyu*, 1934, vol. 11, pp. 461–90.
11. A.R.E. Singer and S.A. Cottrell: *J. Inst. Met.*, 1947, vol. 73, pp. 33–55.
12. C.M. Craighead, E.W. Cawthorne, and R.I. Jaffee: *Trans. AIME*, 1955, vol. 203, pp. 81–87.
13. O. Berthou, G. Petot-Ervas, C. Petot, and P. Desres: *C.R. Acad. Sci. Paris*, 1969, vol. 268C, pp. C1939–42.
14. K. Kobayashi, R.H. Shingu, H. Kanbara, and R. Ozaki: *Trans. Jpn. Inst. Met.*, 1976, vol. 17, pp. 545–50.
15. K. Kobayashi, R.H. Shingu, and R. Ozaki: *Scripta Metall.*, 1976, vol. 10, pp. 525–27.
16. B. Girault, F. Chevrier, A. Joullie, and G. Bougnot: *J. Cryst. Growth*, 1977, vol. 37, pp. 169–77.
17. H. Okamoto: *J. Phase Equil.*, 2007, vol. 28, p. 404.
18. M. Heyrman and P. Chartrand: *J. Phase Equil.*, 2006, vol. 27, pp. 220–30.
19. J. Grobner, I. Chumak, and R. Schmid-Fetzer: *Intermetallics*, 2003, vol. 11, pp. 1065–74.
20. P. Manfrinetti, M.L. Fornasini, and A. Palenzona: *Intermetallics*, 2000, vol. 8, pp. 223–28.
21. E. Schurmann, C. Zellerfeld, H. Litterscheidt, and P. Funders: *Arch. Eisenhüttenwes.*, 1976, vol. 46, pp. 427–32.
22. V.L. Wohler and O. Schliephake: *Z. Anorg. Allg. Chem.*, 1926, vol. 151, pp. 1–20.
23. J.R. Wynnickyj and L.M. Pidgeon: *Metall. Trans.*, 1971, vol. 2, pp. 975–78.
24. S. Tamaru: *Z. Anorg. Allg. Chem.*, 1909, vol. 62, pp. 81–88.
25. H. Feufel, T. Godecke, H.L. Lukas, and F. Sommer: *J. Alloys Compd.*, 1997, vol. 247, pp. 31–42.
26. X. Yan, F. Zhang, and Y.A. Chang: *J. Phase Equilib.*, 2000, vol. 21, pp. 374–84.
27. R. Vogel: *Z. Anorg. Chem.*, 1909, vol. 61, pp. 46–63.
28. R. Geffken and E. Miller: *Trans. TMS-AIME*, 1968, vol. 242, pp. 2323–28.
29. E. Schurmann and A. Fischer: *Giessereiforschung*, 1977, vol. 29, pp. 111–13.
30. O. Kubaschewski: *Iron-Binary Phase Diagrams*, Springer-Verlag, New York, NY, 1982, pp. 136–38.
31. M. Hansen and K. Anderko: *Constitution of Binary Alloys*, McGraw-Hill, New York, NY, 1958, pp. 711–17.
32. R. Schmid: *CALPHAD*, 1980, vol. 4, pp. 101–08.
33. J.L. Haughton and M.L. Becker: *J. Iron Steel Res. Int.*, 1930, vol. 121, p. 315.
34. J.P. Piton and M.F. Fay: *Acad. Sc. Paris*, 1968, vol. C266, p. 514.
35. J. Lacaze and B. Sundman: *Metall. Trans. A*, 1991, vol. 22A, pp. 2211–23.
36. F.A. Shunk: *Constitution of Binary Alloys, 2nd Supplement*, McGraw-Hill, New York, NY, 1985, pp. 347–48.
37. J. Safarian and M. Tangstad: unpublished research, 2010.
38. M. Hansen, H.D. Kessler, and D.J. McPherson: *Trans. Am. Soc. Met.*, 1952, vol. 44, pp. 518–38.
39. V.N. Sovechnikov, Y.A. Kocherzhisky, L.M. Yupko, O.G. Kulik, and E.A. Shishkin: *Dokl. Akad. Nauk SSSR*, 1970, vol. 193, pp. 393–96.
40. J.L. Murray: *Phase Diagrams of Binary Titanium Alloys*, ASM, Materials Park, OH, 1987, pp. 289–94.
41. C. Vahlas, P.Y. Chevalier, and E. Blanquet: *CALPHAD*, 1989, vol. 13, pp. 273–92.
42. H.J. Seifert, H.L. Lukas, and G. Petzow: *Z. Metallkd.*, 1996, vol. 87, pp. 2–13.
43. A. Shukla, Y. Kang, and A.D. Pelton: *CALPHAD*, 2008, vol. 32, pp. 470–77.
44. H. Moissan and F. Siemens: *Acad. Sci. Paris*, 1904, vol. 138, p. 657.
45. M. Schneider and M. Krumnacker: *Neue Hutte*, 1972, vol. 17, pp. 519–21.
46. M. John, K. Hein, and E. Buhrig: *Kristall und Technik*, 1979, vol. 14, pp. 841–48.
47. R.W. Olesinski and G.J. Abbaschian: *Bull. Alloy Phase Diagr.*, 1985, vol. 6, pp. 545–47.
48. R.W. Olesinski and G.J. Abbaschian: *Bull. Alloy Phase Diagr.*, 1986, vol. 7, pp. 170–78.
49. X. Yan and Y.A. Chang: *J. Alloys Compd.*, 2000, vol. 308, pp. 221–29.
50. E. Rudolphi: *Zeitschr. Anorg. Chem.*, 1907, vol. 53, pp. 216–29.
51. M. Hansen and K. Anderko: *Constitution of Binary Alloys*, McGraw-Hill, New York, NY, 1958, pp. 629–33.
52. C.S. Smith: *Trans. AIME*, 1929, vol. 83, pp. 414–39.
53. R.W. Olesinski, A.B. Gokhale, and G.J. Abbaschian: *Bull. Alloy Phase Diagr.*, 1989, vol. 10, pp. 635–39.
54. P.Y. Chevalier: *Thermochim. Acta*, 1988, vol. 130, pp. 33–41.
55. G. Arrivant: *C.R. Hebd. Seances Acad. Sci.*, 1908, vol. 147, pp. 859–61.
56. J.P. Hager: *Trans. TMS-AIME*, 1963, vol. 227, pp. 1000–02.
57. P. Mournon and G. Vuillard: *C.R. Hebd. Seances Acad. Sci.*, 1969, vol. 269, pp. 595–98.
58. B. Predel and H. Bankstahl: *J. Less Common Met.*, 1975, vol. 43, pp. 191–203.
59. R.P. Elliot and F.A. Shunk: *Bull. Alloy Phase Diagr.*, 1981, vol. 2, pp. 359–62.
60. P.Y. Chevalier: *Thermochim. Acta*, 1989, vol. 141, pp. 217–26.
61. H. Okamoto and T.B. Massalski: *Bull. Alloy Phase Diagr.*, 1983, vol. 4, pp. 190–98.
62. C. Di: *Capua: RC. Accad. Naz. Lincei*, 1920, vol. 29, p. 111.
63. E.G. Heath: *J. Electron Control*, 1961, vol. 11, pp. 13–15.
64. W. Gerlach and B. Goel: *Solid-State Electronics*, Pergamon Press, Oxford, UK, 1967, vol. 10, pp. 5–592.
65. L.L. Xu, J. Wang, H.S. Liu, and Z.P. Jin: *CALPHAD*, 2008, vol. 32, pp. 101–05.
66. N.M. Voronov: *Izv. Sekt. Platiny*, 1936, vol. 13, pp. 145–66.
67. R. Massara and P. Feschotte: *J. Alloys Compd.*, 1993, vol. 201, pp. 223–27.
68. R.W. Olesinski and G.J. Abbaschian: *Bull. Alloy Phase Diagr.*, 1984, vol. 5, pp. 273–76.
69. M.H.G. Jacobs and P.J. Spencer: *CALPHAD*, 1996, vol. 20, pp. 89–91.
70. C. Tamaru: *Z. Anorg. Allg. Chem.*, 1909, vol. 69, pp. 40–45.
71. F.A. Trumbore, C.R. Isenberg, and E.M. Porbansky: *J. Phys. Chem. Solids*, 1958, vol. 9, pp. 60–69.
72. A.N. Kobylkin, S.B. Maslenkov, A.G. Nikolaev, and B.I. Nayashkov: *Zavod Lab.*, 1982, vol. 48, pp. 376–79.
73. R.W. Olesinski and G.J. Abbaschian: *Bull. Alloy Phase Diagr.*, 1984, vol. 5, pp. 271–73.
74. R.W. Olesinski and G.J. Abbaschian: *Bull. Alloy Phase Diagr.*, 1985, vol. 6, pp. 359–61.
75. R.S. Williams: *Z. Anorg. Chem.*, 1907, vol. 55, pp. 1–33.
76. R.W. Olesinski and G.J. Abbaschian: *Bull. Alloy Phase Diagr.*, 1985, vol. 6, pp. 445–48.
77. Y. Malmeja, P. Desre, and E. Bonnier: *Mem. Sci. Rev. Metall.*, 1972, vol. 69, pp. 565–77.
78. R.W. Olesinski, N. Kanani, and G.J. Abbaschian: *Bull. Alloy Phase Diagr.*, 1985, vol. 6, pp. 362–64.
79. W. Klemm, L. Klemm, F. Hohmann, H. Volk, E. Orlaumunder, and H.A. Klein: *Z. Anorg. Allg. Chem.*, 1948, vol. 256, pp. 239–52.
80. P.H. Keck and J. Broder: *Phys. Rev. Lett.*, 1953, vol. 90, pp. 521–22.
81. Y.M. Savitskiy, V.V. Baron, and M.A. Tylkina: *Russ. J. Inorg. Chem.*, 1958, vol. 3, pp. 310–27.
82. R.W. Olesinski, N. Kanani, and G.J. Abbaschian: *Bull. Alloy Phase Diagr.*, 1985, vol. 6, pp. 128–30.
83. H. Okamoto: *J. Phase Equilib.*, 2007, vol. 28, pp. 231–32.
84. Z. Du, C. Guo, Z. Yang, and T. Liu: *Intermetallics*, 2006, vol. 14, pp. 560–69.
85. H. Langer and E. Wachtel: *Z Metallkd.*, 1981, vol. 72, pp. 769–75.

86. R. Massara and P. Feschotte: *J. Alloys Compd.*, 1993, vol. 190, pp. 249–54.
87. N.K. Rao and H. Winterhager: *Trans. Indian Inst. Met.*, 1956, vol. 10, p. 139.
88. K. Tsumori and H. Akimune: *J. Mater. Sci.*, 1990, vol. 25, pp. 1479–86.
89. K. Iwase and M. Okamoto: *Sci. Rep. Tohoku Imp. Univ., K. Honda Anniv.*, vol. 936, pp. 777–92.
90. P. Nash and A. Nash: *Bull. Alloy Phase Diagr.*, 1987, vol. 8, pp. 6–14.
91. T. Tokunaga, K. Nishio, H. Ohtani, and M. Hasebe: *CALPHAD*, 2003, vol. 27, pp. 161–68.
92. Y. Du and J.C. Schuster: *Metall. Mater. Trans. A*, 1999, vol. 30A, pp. 2409–18.
93. F. Doerinkel: *Z. Anorg. Chem.*, 1906, vol. 50, pp. 115–26.
94. L.D. Dudkin and E.S. Kuznetsova: *Dokl. AN SSSR*, 1961, vol. 141, pp. 94–97.
95. M.A. Morokhovets, E.I. Elagina, and N.K. Abrikosov: *Neorg. Mater.*, 1966, vol. 2, pp. 561–65.
96. V.T. Mager and E. Wachtel: *Z. Metallkde*, 1970, vol. 61, pp. 853–56.
97. Y. Fujino, D. Shinoda, and S. Asanabe: *Jpn. J. App. Phys.*, 1964, vol. 3, pp. 431–35.
98. A.-B. Gokhale and R. Abbaschian: *Bull. Alloy Phase Diagr.*, 1990, vol. 11, pp. 468–75.
99. H. Okamoto: *J. Phase Equilib.*, 1991, vol. 12, pp. 505–07.
100. N. Chakraborti and H. Lukas: *CALPHAD*, 1989, vol. 13, pp. 293–300.
101. P.-Y. Chevalier, E. Fischer, and A. Rivet: *CALPHAD*, 1995, vol. 19, pp. 57–68.
102. L. Schellenberg, J.L. Jorda, and J. Muller: *J. Less Common Met.*, 1985, vol. 109, pp. 261–74.
103. L.M. Yupko: *Dokl. Akad. Nauk SSSR*, 1987, vol. 296, pp. 100–02.
104. M.E. Schlesinger: *J. Phase Equilib.*, 1992, vol. 13, pp. 54–59.